Real Stueckelberg Quantum Geometry and Unbroken Supersymmetry in the Rotating Shallow Water Model

Andrei Galiautdinov *

Posted Date: 9 May 2026

doi: 10.20944/preprints202605.0606.v1

Keywords: topological fluid dynamics; rotating shallow water model; rotating shallow equations; equatorial waves; Coriolis parameter; Kelvin and Yanai modes; Poincare waves; Rossby waves; Stueckelberg real quantum mechanics; Fubini-Study metric; Berry phase; Berry connection; Berry curvature; supersymmetry; Witten index

 doi:10.20944/preprints202605.0606.v1

Article

Real Stueckelberg Quantum Geometry and Unbroken Supersymmetry in the Rotating Shallow Water Model

Andrei Galiautdinov

Department of Physics and Astronomy, University of Georgia, Athens, Georgia 30602, USA; ag1@uga.edu

Abstract

The topological properties of planetary fluids are typically analyzed by mapping classical fluid equations onto complex quantum mechanical models. Here we present a purely real, six-dimensional Stueckelberg quantum mechanical formulation of the rotating shallow water equations to demonstrate that these topological features are intrinsic to the classical kinematics itself. Operating entirely within $\mathbb{R}^6$, we decouple the complex quantum geometric tensor into an independent, real Fubini-Study metric and a real antisymmetric Berry curvature. Our real-variable approach explicitly derives a topological magnetic monopole of charge $C = 2$ and captures the inherent scale invariance of the fluid's geometry without the need for complexification. We suggest that continuous variations in the Coriolis parameter may dynamically model the deep-time planetary evolution of the Archean Earth, and we propose a laboratory rotating-tank experiment to physically measure this topological phase transition. Finally, we show that our real 6D formulation naturally maps to unbroken supersymmetric quantum mechanics. By identifying a purely real supercharge and calculating a fluid Witten index of $W = -2$, we advance a mathematically supported viewpoint that steady-state geostrophic weather patterns represent the unbroken, zero-energy supersymmetric ground states of the rotating fluid system. Consequently, the topological isolation of this vacuum naturally restricts the spectral flow across the equator, providing a theoretical explanation for the unidirectional eastward motion of equatorial boundary waves.

Keywords: topological fluid dynamics; rotating shallow water model; rotating shallow equations; equatorial waves; Coriolis parameter; Kelvin and Yanai modes; Poincare waves; Rossby waves; Stueckelberg real quantum mechanics; Fubini-Study metric; Berry phase; Berry connection; Berry curvature; supersymmetry; Witten index

1. Introduction

In recent years, concepts from topological band theory that were originally used in solid-state physics [1,2] have been applied to classical fluids. In planetary oceans and atmospheres, the planet's rotation breaks time-reversal symmetry, creating a frequency gap between slow geostrophic weather patterns and fast gravity waves. As first established by Delplace *et al.* [3–5], building upon the foundational work by Matsuno [6], this gap topologically guarantees the emergence of special boundary states, such as equatorial Kelvin waves [7], which are forced to travel in only one direction along the equator.

To analyze these phenomena, standard models intrinsically rely on mapping classical equations into complex mathematical spaces, a technique previously adopted in classical topological mechanics and acoustics (e.g., [8,9]). Of particular importance to us is the recent work by Ganeshan and Dorsey [10], who provided a deep theoretical insight into the nature of the subject by mapping the rotating shallow water equations to a complex pseudo-spin-1 system in an artificial magnetic field. Since this beautiful theoretical approach bypasses the fact that classical fluids are fundamentally real, a natural question arises as to whether a *comparable*, yet *fully real*, formulation of the rotating shallow water model is possible. This question is pertinent, since, as was already pointed out in the commentary by Biello and Dimofte [11] accompanying the original paper by Delplace *et al.*, relying on complex

 doi:10.20944/preprints202605.0606.v1

wavefunctions leaves open various important conceptual issues, such as whether topological winding numbers simply cancel out when combining them to form real-valued physical waves.

In this paper, we propose an approach based on a purely real, six-dimensional Stueckelberg formulation of quantum mechanics [12]. By keeping all calculations within $\mathbb{R}^6$, we show that the topological features of planetary waves come directly from the standard classical equations, without needing complex variables.

We provide the purely real formulation of the quantum geometric tensor [13] (also [14–17]) and derive its two independent, real parts: a symmetric Fubini-Study metric [18,19] and an antisymmetric Berry curvature [20]. Using real components, we re-derive a topological magnetic monopole with a charge of $C = 2$. This demonstrates that real classical superpositions do not suffer from topological cancellation; the winding arises from the real symplectic kinematics of the fluid, rather than an imaginary phase.

We also connect our formulation to physical reality, for instance, regarding a change in the rotation parameter f as analogous to looking at the Earth billions of years ago when it rotated faster. We propose a laboratory rotating tank experiment that gradually slows down to provide a practical way to observe these geometric changes in real time.

Additionally, we show that this real 6D model shares the mathematical structure of supersymmetric quantum mechanics (SUSY QM) [21–23] (cf. [24]). Within this interpretation, the main dynamical Hamiltonian of the rotating shallow water equations acts as a purely real supercharge, $\mathcal{Q}$, while the formal supersymmetric Hamiltonian is generated by its square, $\mathcal{H} = \mathcal{Q}^2$. By utilizing the inherent spatial parity differences between the scalar height and vector velocity fields we calculate a Witten index of $W = -2$.[1] Rather than indicating two distinct physical phenomena, this integer protects a doubly degenerate zero-frequency subspace, corresponding to the orthogonal sine and cosine spatial quadratures of a single continuous geostrophic balance. This guarantees the perpetual existence of stable large-scale geostrophic weather patterns on a rotating planet. Also, this unbroken classical vacuum structure fulfills the topological role traditionally played by a filled Fermi sea in quantum systems. Its topological isolation restricts the spectral flow across the equator, naturally forcing the observed boundary states to propagate exclusively eastward.

Finally, to explicitly demonstrate how this bulk topology governs the physical fluid boundaries, Appendix A we re-derive Matsuno's equatorial edge states (the Kelvin and Yanai waves) entirely within our real Stueckelberg formulation.

2. Real Quantum Geometry via Stueckelberg Formalism

The usual derivations of the quantum geometric tensor rely on a complex Hilbert space. Because macroscopic classical fluid fields are real-valued quantities, we apply the 1960 method by Stueckelberg [12], which showed that quantum mechanics can be alternatively formulated over a real Hilbert space. This is achieved by introducing an antisymmetric super-selection operator J satisfying the algebraic condition $J^2 = -I$.

2.1. Rotating Shallow Water System and Dispersion Relations

The state of the fluid system is described by a real vector field

$$\Psi(\boldsymbol{x}, t) = (u, v, \eta)^T = \begin{pmatrix} u \\ v \\ \eta \end{pmatrix}, \tag{1}$$

[1] Recently, Tong [25] provided a powerful complementary perspective by reformulating the rotating shallow water equations as a macroscopic $2+1$-dimensional Abelian gauge theory. In that approach, the kinematic differences between the scalar height and vector velocity fields are captured by mapping them to magnetic and electric fields, respectively. This allows the linearised Poincaré waves to be modeled via Maxwell-Chern-Simons theory and identifies coastal Kelvin waves as chiral gauge edge modes. While Tong exposes the fluid's topological nature through via continuous real-space effective field theory, and Ganeshan & Dorsey [10] do so via momentum-space Berry curvature, our 6D real formulation reveals the exact same underlying reality through the local algebraic description via supersymmetric quantum mechanics and the Witten index.

 doi:10.20944/preprints202605.0606.v1

where $u(\boldsymbol{x},t)$ and $v(\boldsymbol{x},t)$ represent the zonal and meridional horizontal velocity anomalies, and $\eta(\boldsymbol{x},t)$ represents the free-surface height anomaly [26,27]. Following standard dimensional re-scaling [3] (also [10]), we define the non-dimensionalized variables (denoted with tildes),

$$v = c\tilde{v}, \quad u = c\tilde{u}, \quad \eta = H\tilde{\eta}, \quad x = L_d\tilde{x}, \quad y = L_d\tilde{y}, \quad t = \frac{\tilde{t}}{2\Omega}, \quad f = 2\Omega\tilde{f}, \tag{2}$$

where the characteristic velocity and length scales of the fluid system are defined by

$$c^2 = gH, \quad L_d = \frac{c}{2\Omega}. \tag{3}$$

Here, $f = 2\Omega\sin\vartheta$ is the Coriolis parameter (with ϑ being the latitude measured from the equator), g denotes the gravitational acceleration, and H stands for the mean depth of the unperturbed fluid. Dropping the tildes for notational simplicity, the linearized rotating shallow water equations take the form,

$$\partial_t\Psi = L_{\text{sp}}\Psi, \tag{4}$$

where

$$L_{\text{sp}} = \begin{pmatrix} 0 & f & -\partial_x \\ -f & 0 & -\partial_y \\ -\partial_x & -\partial_y & 0 \end{pmatrix} \tag{5}$$

is the real spatial differential operator.

We next construct an explicitly real propagating plane wave solution to the fluid equations as a superposition of two quadratures,

$$\Psi(\boldsymbol{x},t) = \Psi_1(\boldsymbol{k})\cos(\boldsymbol{k}\cdot\boldsymbol{x} - \omega(\boldsymbol{k})t) + \Psi_2(\boldsymbol{k})\sin(\boldsymbol{k}\cdot\boldsymbol{x} - \omega(\boldsymbol{k})t), \tag{6}$$

where $\Psi_1(\boldsymbol{k})$ and $\Psi_2(\boldsymbol{k})$ are appropriately chosen three-dimensional real column vectors. Substituting into Eq. (4) and using (5), after some algebra we find the system,

$$\omega(\boldsymbol{k})\Psi_1 = -K\Psi_1 + F\Psi_2, \quad -\omega(\boldsymbol{k})\Psi_2 = F\Psi_1 + K\Psi_2, \tag{7}$$

with

$$F = \begin{pmatrix} 0 & f & 0 \\ -f & 0 & 0 \\ 0 & 0 & 0 \end{pmatrix} = -F^{\text{T}}, \quad K = \begin{pmatrix} 0 & 0 & -k_x \\ 0 & 0 & -k_y \\ -k_x & -k_y & 0 \end{pmatrix} = K^{\text{T}}, \tag{8}$$

which may be re-written in the 6×6 matrix form,

$$\begin{pmatrix} F & K \\ -K & F \end{pmatrix}\begin{pmatrix} \Psi_1 \\ \Psi_2 \end{pmatrix} = \omega(\boldsymbol{k})\begin{pmatrix} 0 & -I_3 \\ I_3 & 0 \end{pmatrix}\begin{pmatrix} \Psi_1 \\ \Psi_2 \end{pmatrix}. \tag{9}$$

Defining the 6×6 matrices,

$$\mathcal{G} = \begin{pmatrix} F & K \\ -K & F \end{pmatrix}, \quad \mathcal{J} = \begin{pmatrix} 0 & -I_3 \\ I_3 & 0 \end{pmatrix}, \tag{10}$$

we see that

$$\mathcal{J}^{\text{T}} = -\mathcal{J}, \quad \mathcal{J}^2 = -I_6, \quad \mathcal{G}^{\text{T}} = -\mathcal{G}, \quad [\mathcal{G},\mathcal{J}] = 0, \tag{11}$$

with $\mathcal{J}$ functioning as the imaginary unit i, while $\mathcal{G}$ being antisymmetric. Multiplying by $(-\mathcal{J})$ on the left, Eq. (9) becomes

$$\mathcal{M}\begin{pmatrix} \Psi_1 \\ \Psi_2 \end{pmatrix} = \begin{pmatrix} 0 \\ 0 \end{pmatrix}, \tag{12}$$

 doi:10.20944/preprints202605.0606.v1

with

$$\mathcal{M} = \begin{pmatrix} -K-\omega(\boldsymbol{k}) & F \\ -F & -K-\omega(\boldsymbol{k}) \end{pmatrix} = \begin{pmatrix} -\omega(\boldsymbol{k}) & 0 & k_x & 0 & f & 0 \\ 0 & -\omega(\boldsymbol{k}) & k_y & -f & 0 & 0 \\ k_x & k_y & -\omega(\boldsymbol{k}) & 0 & 0 & 0 \\ 0 & -f & 0 & -\omega(\boldsymbol{k}) & 0 & k_x \\ f & 0 & 0 & 0 & -\omega(\boldsymbol{k}) & k_y \\ 0 & 0 & 0 & k_x & k_y & -\omega(\boldsymbol{k}) \end{pmatrix}, \tag{13}$$

whose determinant is

$$\det(\mathcal{M}) = \omega(\boldsymbol{k})^2 (k_x^2 + k_y^2 + f^2 - \omega(\boldsymbol{k})^2)^2, \tag{14}$$

resulting in the dispersion relations for the three frequency bands,

$$\omega_0(\boldsymbol{k}) = 0, \quad \omega_+(\boldsymbol{k}) = \omega, \quad \omega_-(\boldsymbol{k}) = -\omega, \tag{15}$$

where

$$\omega \equiv +\sqrt{k_x^2 + k_y^2 + f^2}. \tag{16}$$

2.2. Connection to Stueckelberg's Real Hilbert Space Formulation

The emergence of the 6×6 algebraic system in Eq. (9) reveals a deep structural isomorphism between the classical fluid dynamics and Ernst Stueckelberg's formulation of quantum mechanics in a real Hilbert space. Stueckelberg demonstrated that the imaginary unit i is not necessary for formulating quantum theory, provided the real state space is equipped with a distinguished, antisymmetric, orthogonal operator $\mathcal{J}$ satisfying $\mathcal{J}^2 = -I$.

In our approach, the real six-dimensional state vector Φ is constructed by stacking the two spatial quadratures,

$$\Phi(\boldsymbol{k}) = \begin{pmatrix} \Psi_1(\boldsymbol{k}) \\ \Psi_2(\boldsymbol{k}) \end{pmatrix}. \tag{17}$$

Because Ψ_1 and Ψ_2 act as the real and imaginary parts of a conventional complex wave amplitude, applying the operator $\mathcal{J}$ physically rotates the quadratures by $\pi/2$, mimicking the algebraic operation of multiplying a complex state by i.

In standard complex quantum mechanics, time evolution is generated by a Hermitian Hamiltonian via the Schrödinger equation,

$$i\partial_t \psi = H\psi. \tag{18}$$

In Stueckelberg's real formalism, the time evolution is instead governed by an antisymmetric generator of rotations in the real vector space. Returning to Eq. (9), we have

$$\mathcal{G}\Phi = \omega(\boldsymbol{k})\mathcal{J}\Phi. \tag{19}$$

By multiplying both sides from the left by $(-\mathcal{J})$ and using $\mathcal{J}^2 = -I_6$, we obtain the purely real, symmetric eigenvalue problem,

$$\mathcal{H}_S\Phi = \omega(\boldsymbol{k})\Phi, \tag{20}$$

where $\mathcal{H}_S$ is the real Stueckelberg Hamiltonian, defined by

$$\mathcal{H}_S \equiv -\mathcal{J}\mathcal{G} = \begin{pmatrix} 0 & I_3 \\ -I_3 & 0 \end{pmatrix} \begin{pmatrix} F & K \\ -K & F \end{pmatrix} = \begin{pmatrix} -K & F \\ -F & -K \end{pmatrix} = \begin{pmatrix} 0 & 0 & k_x & 0 & f & 0 \\ 0 & 0 & k_y & -f & 0 & 0 \\ k_x & k_y & 0 & 0 & 0 & 0 \\ 0 & -f & 0 & 0 & 0 & k_x \\ f & 0 & 0 & 0 & 0 & k_y \\ 0 & 0 & 0 & k_x & k_y & 0 \end{pmatrix}. \tag{21}$$

 doi:10.20944/preprints202605.0606.v1

Recalling that $K^{\mathrm{T}} = K$ and $F^{\mathrm{T}} = -F$, we find,

$$\mathcal{H}_S^{\mathrm{T}} = \begin{pmatrix} -K^{\mathrm{T}} & -F^{\mathrm{T}} \\ F^{\mathrm{T}} & -K^{\mathrm{T}} \end{pmatrix} = \begin{pmatrix} -K & F \\ -F & -K \end{pmatrix} = \mathcal{H}_S, \tag{22}$$

verifying that $\mathcal{H}_S$ is symmetric, making it the exact real-space equivalent of a complex Hermitian Hamiltonian. We can now recognize that the matrix $\mathcal{M}$ in Eq. (12) is simply

$$\mathcal{M} = \mathcal{H}_S - \omega(\boldsymbol{k}) I_6, \tag{23}$$

confirming that finding the null space of $\mathcal{M}$ is physically identical to finding the real eigenvectors of the Stueckelberg Hamiltonian.

Following Stueckelberg, we equip our finite-dimensional real space with the standard symmetric Euclidean inner product,

$$\langle \Phi_A, \Phi_B \rangle_{\mathbb{R}} = \Phi_A^{\mathrm{T}} \Phi_B = \sum_{j=1}^{6} (\Phi_A)_j (\Phi_B)_j. \tag{24}$$

Because we have scaled our physical variables with $c^2 = gH$, this real Euclidean metric corresponds to the total conserved mechanical energy of the fluid anomalies. Furthermore, Stueckelberg proved that the geometry of the standard complex inner product is entirely recoverable from this real metric via the relation,

$$\langle A_{\mathbb{C}} | B_{\mathbb{C}} \rangle_{\mathbb{C}} = \langle \Phi_A, \Phi_B \rangle_{\mathbb{R}} - i \langle \Phi_A, \mathcal{J} \Phi_B \rangle_{\mathbb{R}}, \tag{25}$$

where $|A_{\mathbb{C}}\rangle$ and $|B_{\mathbb{C}}\rangle$ are the corresponding complex-valued quantum states. Thus, our six-dimensional real Hilbert space preserves all quantum and geometric information, without the need for complex numbers.

2.3. Real Eigenmodes and Stueckelberg Orthogonality

To complete the formal propagating plane wave solution, we evaluate the null space of $\mathcal{M}$ to extract the eigenmodes for each branch of the dispersion relation. Let us define the magnitude of the horizontal wave vector as

$$k^2 \equiv k_x^2 + k_y^2. \tag{26}$$

Because we are operating in the reals, the arbitrary complex $U(1)$ phase is replaced by an $SO(2)$ kinematic rotational degeneracy between the cosine and sine quadratures. We fix this gauge by setting the height anomaly of the second quadrature to zero,

$$\eta_2 = 0. \tag{27}$$

For the stationary geostrophic branch, $\omega_0 = 0$, the relation $\mathcal{M}\Phi = 0$ yields a two-dimensional null space representing topological zero-modes. The first unnormalized state is then found to be,

$$\Phi_{G1} = \begin{pmatrix} 0 \\ 0 \\ f \\ k_y \\ -k_x \\ 0 \end{pmatrix}. \tag{28}$$

Its orthogonal complement in the degenerate subspace is generated by applying the complex structure operator,

$$\Phi_{G2} = \mathcal{J} \Phi_{G1}. \tag{29}$$

 doi:10.20944/preprints202605.0606.v1

Using the Euclidean inner product, the squared norm of this state is

$$\langle \Phi_{G1}, \Phi_{G1} \rangle_{\mathbb{R}} = 0^2 + 0^2 + f^2 + k_y^2 + (-k_x)^2 + 0^2 = k^2 + f^2. \tag{30}$$

Because $\mathcal{J}$ is an orthogonal operator, $\mathcal{J}^{\mathrm{T}}\mathcal{J} = I_6$, it acts as an isometry, and thus Φ_{G2} possesses the identical norm. The fully normalized geostrophic mode pairs are therefore

$$\hat{\Phi}_{G1} = \frac{1}{\sqrt{k^2+f^2}} \begin{pmatrix} 0 \\ 0 \\ f \\ k_y \\ -k_x \\ 0 \end{pmatrix}, \quad \hat{\Phi}_{G2} = \frac{1}{\sqrt{k^2+f^2}} \begin{pmatrix} -k_y \\ k_x \\ 0 \\ 0 \\ 0 \\ f \end{pmatrix}. \tag{31}$$

For the propagating Poincaré waves, $\omega_\pm \neq 0$, we use the dispersion relation identity $k^2 = \omega^2 - f^2$. Solving $\mathcal{M}\Phi = 0$ yields the primary unnormalized vectors,

$$\Phi_{P1} = \begin{pmatrix} \omega k_x \\ \omega k_y \\ k^2 \\ -f k_y \\ f k_x \\ 0 \end{pmatrix}, \quad \Phi_{N1} = \begin{pmatrix} -\omega k_x \\ -\omega k_y \\ k^2 \\ -f k_y \\ f k_x \\ 0 \end{pmatrix}. \tag{32}$$

Taking the inner product of, say, Φ_{P1} with itself, we find

$$\langle \Phi_{P1}, \Phi_{P1} \rangle_{\mathbb{R}} = \omega^2 k^2 + k^4 + f^2 k^2 = k^2(\omega^2 + k^2 + f^2) = 2k^2\omega^2. \tag{33}$$

Defining the normalization factor, $\mathcal{N} = \sqrt{2}k\omega$, the fully normalized propagating positive-frequency eigenmodes are

$$\hat{\Phi}_{P1} = \frac{1}{\sqrt{2}k\omega} \begin{pmatrix} \omega k_x \\ \omega k_y \\ k^2 \\ -f k_y \\ f k_x \\ 0 \end{pmatrix}, \quad \hat{\Phi}_{P2} = \frac{1}{\sqrt{2}k\omega} \begin{pmatrix} f k_y \\ -f k_x \\ 0 \\ \omega k_x \\ \omega k_y \\ k^2 \end{pmatrix}, \tag{34}$$

where $\hat{\Phi}_{P2} = \mathcal{J}\hat{\Phi}_{P1}$. Similarly, the negative-frequency eigenmodes are

$$\hat{\Phi}_{N1} = \frac{1}{\sqrt{2}k\omega} \begin{pmatrix} -\omega k_x \\ -\omega k_y \\ k^2 \\ -f k_y \\ f k_x \\ 0 \end{pmatrix}, \quad \hat{\Phi}_{N2} = \frac{1}{\sqrt{2}k\omega} \begin{pmatrix} f k_y \\ -f k_x \\ 0 \\ -\omega k_x \\ -\omega k_y \\ k^2 \end{pmatrix}, \tag{35}$$

where $\hat{\Phi}_{N2} = \mathcal{J}\hat{\Phi}_{N1}$. Because the classical fluid system possesses a particle-hole-like symmetry, the geometric and topological properties of this latter negative branch are symmetric to those of the positive branch. Therefore, we restrict our subsequent geometric analysis to the positive-frequency modes and the geostrophic zero-modes. Together, these are sufficient to fully characterize the topological invariants of the system while ensuring the mathematical completeness of the $\mathbb{R}^6$ basis.

 doi:10.20944/preprints202605.0606.v1

Finally, a fundamental requirement of our basis is that these degenerate pairs must be orthogonal. We verify this by exploiting the inherent antisymmetric nature of $\mathcal{J}$. For any real normalized state $\hat{\Phi}$ and its Stueckelberg partner $\mathcal{J}\hat{\Phi}$, their Euclidean inner product is given by the quadratic form,

$$\langle \hat{\Phi}, \mathcal{J}\hat{\Phi} \rangle_{\mathbb{R}} = \hat{\Phi}^{\mathrm{T}} \mathcal{J} \hat{\Phi}. \tag{36}$$

Because $\mathcal{J}^{\mathrm{T}} = -\mathcal{J}$, the corresponding real quadratic form vanishes for all states. This guarantees that

$$\langle \hat{\Phi}_{G1}, \hat{\Phi}_{G2} \rangle_{\mathbb{R}} = 0, \quad \langle \hat{\Phi}_{P1}, \hat{\Phi}_{P2} \rangle_{\mathbb{R}} = 0, \quad \langle \hat{\Phi}_{N1}, \hat{\Phi}_{N2} \rangle_{\mathbb{R}} = 0, \tag{37}$$

securing an orthonormal basis for the real Hilbert space construction without relying on complex conjugation.

2.4. General Solution

With the complete set of normalized, mutually orthogonal six-dimensional eigenmodes secured, we can now map these states back to physical space to construct the general spatial-temporal solution, $\Psi(\boldsymbol{x}, t)$, for the original three-component planetary fluid system governed by Eq. (4).

Recall that the six-dimensional real state vector separates the harmonic quadratures, storing the cosine amplitudes in the upper three components and the sine amplitudes in the lower three components. We can formalize the return to the physical three-dimensional wave field by defining a 3×6 phase projection operator,

$$\mathcal{P}(\theta) = \begin{pmatrix} \cos\theta\, I_3 & \sin\theta\, I_3 \end{pmatrix}, \tag{38}$$

where I_3 is the 3×3 identity matrix, and θ is the standard kinematic phase argument. For any given dynamical branch $b \in \{G, P, N\}$, this phase angle is defined as

$$\theta_b(\boldsymbol{k}, \boldsymbol{x}, t) = \boldsymbol{k} \cdot \boldsymbol{x} - \omega_b(\boldsymbol{k}) t, \tag{39}$$

where the respective frequencies for each branch are the stationary geostrophic mode $\omega_0 = 0$, the positive Poincaré mode $\omega_+ = \sqrt{k^2 + f^2}$, and the negative Poincaré mode $\omega_- = -\sqrt{k^2 + f^2}$.

Because the Stueckelberg partners $\hat{\Phi}_{b1}(\boldsymbol{k})$ and $\hat{\Phi}_{b2}(\boldsymbol{k})$ span the complete orthogonal degenerate subspace for each branch at a specified wave vector $\boldsymbol{k}$, an arbitrary fluid excitation is simply a real linear combination of these two basis states. Integrating over all possible continuous wave vectors and summing over the three dynamical branches, the most general physical solution takes the form

$$\Psi(\boldsymbol{x}, t) = \int \frac{d^2k}{(2\pi)^2} \sum_{b \in \{G,P,N\}} \mathcal{P}(\theta_b) \Big[c_{b1}(\boldsymbol{k}) \hat{\Phi}_{b1}(\boldsymbol{k}) + c_{b2}(\boldsymbol{k}) \hat{\Phi}_{b2}(\boldsymbol{k}) \Big]. \tag{40}$$

Here, $c_{b1}(\boldsymbol{k})$ and $c_{b2}(\boldsymbol{k})$ are *real* scalar amplitude distributions, uniquely determined by the initial boundary conditions of the fluid system.

This continuous formulation highlights the mechanical elegance of the real Stueckelberg approach. By substituting the relation $\hat{\Phi}_{b2} = \mathcal{J}\hat{\Phi}_{b1}$, we can observe how the complex structure operator interacts with the spatial phase projector. If we partition the primary state into its upper and lower three-dimensional blocks as $\hat{\Phi}_{b1} = (\Psi_1, \Psi_2)^{\mathrm{T}}$, the action of $\mathcal{J}$ yields $(-\Psi_2, \Psi_1)^{\mathrm{T}}$. Applying the projector to this partnered state gives,

$$\mathcal{P}(\theta)\mathcal{J}\hat{\Phi}_{b1} = \begin{pmatrix} \cos\theta\, I_3 & \sin\theta\, I_3 \end{pmatrix} \begin{pmatrix} -\Psi_2 \\ \Psi_1 \end{pmatrix} = \sin\theta\, \Psi_1 - \cos\theta\, \Psi_2. \tag{41}$$

This operation is equivalent to applying a continuous $\pi/2$ phase shift to the original real-valued wave. Thus, linearly mixing the two real orthogonal states via the continuous scalar coefficients c_{b1} and c_{b2} replicates the rotational utility of an arbitrary complex amplitude $Ae^{i\phi}$. It reproduces the

 doi:10.20944/preprints202605.0606.v1

full spectrum of the fluid's kinematics entirely within the $\mathbb{R}^6$ domain, eliminating the necessity of introducing complex wave fields.

2.5. Comparison with the Complex Formalism

Before proceeding to the computation of the geometric tensor, it is instructive to further compare the real Stueckelberg approach developed above with the standard three-dimensional complex formulation.

In the complex formulation, the wave solutions to the physical equations of motion, Eq. (4), are constructed by employing a complex plane wave Ansatz,

$$\Psi_{\mathbb{C}}(\boldsymbol{x}, t) = \tilde{\Psi} e^{i(\boldsymbol{k}\cdot\boldsymbol{x} - \omega(\boldsymbol{k})t)}, \tag{42}$$

where $\tilde{\Psi} \in \mathbb{C}^3$ is a three-dimensional complex amplitude vector. Under this Ansatz, the real spatial differential operator

$$L_{\mathrm{sp}} = F + D \tag{43}$$

transforms into the 3×3 complex matrix,

$$L_{\mathbb{C}} = F + iK. \tag{44}$$

The time evolution then requires

$$-i\omega(\boldsymbol{k})\tilde{\Psi} = (F + iK)\tilde{\Psi}, \tag{45}$$

which may be re-arranged into a standard Hermitian-like eigenvalue problem in $\mathbb{C}^3$.

Mathematically, the complex three-dimensional eigenvalue problem and the real six-dimensional eigenvalue problem in Eq. (9) are isomorphic. By identifying the complex amplitude as

$$\tilde{\Psi} = \Psi_1 - i\Psi_2, \tag{46}$$

the operation $(F + iK)(\Psi_1 - i\Psi_2)$ naturally reproduces the block matrix dynamics of our $\mathcal{G}$ operator. The efficiency and elegance of the complex formulation make it a powerful computational tool for extracting topological fluid invariants. However, from a physical standpoint, applying the complex formulation to a macroscopic classical fluid introduces subtle interpretive challenges that the real formulation inherently obviates.

First, the complex state $\tilde{\Psi}$ is defined up to an arbitrary local phase $e^{i\chi}$, reflecting the fundamental $U(1)$ gauge symmetry of complex quantum mechanics. In a macroscopic fluid, however, an abstract complex phase has no direct physical meaning. The Stueckelberg formulation clarifies that this $U(1)$ gauge freedom is not an abstract unobservable; it is mathematically identical to the $SO(2)$ kinematic rotational symmetry between the real, observable cosine and sine spatial quadratures of the wave. The "gauge choice" in the real formulation simply corresponds to defining the spatial origin (a phase shift) of the wave coordinate system.

Second, the complex formulation relies on the standard Hermitian inner product on $\mathbb{C}^3$ to derive the Fubini-Study metric and the Berry curvature. As demonstrated in the previous section, the Stueckelberg synthesis unpacks this complex inner product into two distinct real components: a symmetric Euclidean dot product and an antisymmetric form mediated by the complex structure operator $\mathcal{J}$. This separation physically reinterprets the quantum geometry. The symmetric part represents the classical mechanical energy (inertia) of the fluid wave, while the antisymmetric part represents the symplectic area of the classical phase space.

Consequently, the real geometry formulation confirms that the topological features of the fluid are not mathematical artifacts generated by embedding the system into a complex vector space. Rather, the quantum-like geometry is an intrinsic property of the classical Newtonian kinematics of the rotating shallow water model.

 doi:10.20944/preprints202605.0606.v1

3. The Real Quantum Geometric Tensor

To investigate the topological properties of the fluid system, we must examine how the physical eigenmodes vary across the parameter space. Physically, for a wave packet propagating in a fluid at a fixed latitude, the active parameter space is the two-dimensional momentum space, parameterized by the continuous wavevector $\boldsymbol{k} = (k_x, k_y)$. However, to fully reveal the topological structure of the dispersion bands (specifically, the existence of a Dirac-like degeneracy at the origin where the band gap closes) it is mathematically advantageous to elevate the background Coriolis parameter f to the status of a continuous control variable.

Following the insight of Ganeshan and Dorsey [10], who treat f analogously to a varying mass term in the two-dimensional Dirac equation, we formally extend our parameter space to the three-dimensional vector $\boldsymbol{p} = (k_x, k_y, f)$. We define the corresponding parametric derivatives as $\partial_\mu \equiv \partial/\partial p_\mu$, where the indices now span $\mu, \nu \in \{k_x, k_y, f\}$.

In the complex formulation by Ganeshan and Dorsey, the geometric properties of a specific energy band are entirely encoded in the Quantum Geometric Tensor (QGT), constructed using the complex inner product and the band projector $P_{\mathbb{C}} = |\psi\rangle\langle\psi|$. In our real Stueckelberg formulation, we must construct an equivalent geometric tensor using exclusively the six-dimensional real state vectors and the real Euclidean inner product.

Consider a specific dispersion branch (either geostrophic or propagating) spanned by the degenerate, orthonormal 6D state pair $\{\hat{\Phi}_1, \hat{\Phi}_2\}$, where $\hat{\Phi}_2 = \mathcal{J}\hat{\Phi}_1$. The orthogonal projector $P(\boldsymbol{p})$ onto this two-dimensional real subspace is defined as

$$P(\boldsymbol{p}) = \hat{\Phi}_1\hat{\Phi}_1^{\mathrm{T}} + \hat{\Phi}_2\hat{\Phi}_2^{\mathrm{T}} = \hat{\Phi}_1\hat{\Phi}_1^{\mathrm{T}} + \mathcal{J}\hat{\Phi}_1\hat{\Phi}_1^{\mathrm{T}}\mathcal{J}^{\mathrm{T}}. \tag{47}$$

This projector is manifestly gauge-invariant; it depends only on the physical subspace and is invariant under any $SO(2)$ rotation between the quadratures $\hat{\Phi}_1$ and $\hat{\Phi}_2$.

Using the Stueckelberg synthesis of the complex inner product from Sec. 2.2, we can define the Real Quantum Geometric Tensor (RQGT), $\mathcal{T}_{\mu\nu}$, by taking the derivatives of the primary quadrature state $\hat{\Phi}_1$ and projecting out the components that remain within the band,

$$\mathcal{T}_{\mu\nu} = \langle \partial_\mu\hat{\Phi}_1, (I_6 - P)\partial_\nu\hat{\Phi}_1\rangle_{\mathbb{R}} - i\langle \partial_\mu\hat{\Phi}_1, \mathcal{J}(I_6 - P)\partial_\nu\hat{\Phi}_1\rangle_{\mathbb{R}}, \tag{48}$$

where I_6 is the 6×6 identity matrix. Note that we have *formally* kept the i here merely as a bookkeeping device to separate the symmetric and antisymmetric real bilinear forms.

The real part of $\mathcal{T}_{\mu\nu}$ is symmetric under the exchange of indices $\mu \leftrightarrow \nu$. This defines the real formulation of the Fubini-Study metric, $g_{\mu\nu}$, which measures the invariant infinitesimal distance between fluid states in the extended parameter space,

$$g_{\mu\nu} = (\partial_\mu\hat{\Phi}_1)^{\mathrm{T}}(I_6 - P)(\partial_\nu\hat{\Phi}_1). \tag{49}$$

Because $g_{\mu\nu}$ relies solely on the symmetric Euclidean inner product, its physical interpretation is straightforward: it quantifies the sensitivity of the fluid's classical kinetic and potential energy to variations in the wavevector and the background rotation, after subtracting any trivial kinematic rotations within the degenerate band.

The imaginary component of Eq. (48) captures the antisymmetric geometry of the parameter space, leading directly to the Berry phase and Berry curvature.

First, we define the real Berry connection (or gauge potential), A_μ, which describes how the phase (the $SO(2)$ angle between the quadratures) twists as we move through parameter space. In complex quantum mechanics, this is

$$A_\mu^{\mathbb{C}} = i\langle\psi|\partial_\mu\psi\rangle. \tag{50}$$

 doi:10.20944/preprints202605.0606.v1

Applying our Stueckelberg mapping, this operation is equivalently implemented by the complex structure operator $\mathcal{J}$,

$$A_\mu = \langle \hat{\Phi}_1, \mathcal{J}\partial_\mu \hat{\Phi}_1 \rangle_{\mathbb{R}} = \hat{\Phi}_1^{\mathrm{T}} \mathcal{J}\partial_\mu \hat{\Phi}_1. \tag{51}$$

To verify that A_μ acts as a proper gauge connection, consider a local $SO(2)$ gauge transformation (a redefinition of the wave's spatial origin), which rotates the state by an arbitrary parameter-dependent angle $\alpha(\boldsymbol{p})$,

$$\hat{\Phi}_1' = \cos\alpha\, \hat{\Phi}_1 + \sin\alpha\, \hat{\Phi}_2 = \cos\alpha\, \hat{\Phi}_1 + \sin\alpha\, \mathcal{J}\hat{\Phi}_1. \tag{52}$$

Substituting $\hat{\Phi}_1'$ into Eq. (51), and using the relations $\mathcal{J}^2 = -I_6$, $\mathcal{J}^{\mathrm{T}} = -\mathcal{J}$, and the normalization $\hat{\Phi}_1^{\mathrm{T}}\hat{\Phi}_1 = 1$, we find,

$$A_\mu' = A_\mu - \partial_\mu \alpha. \tag{53}$$

This confirms that A_μ transforms exactly like a $U(1)$ Abelian gauge field, derived purely from classical fluid kinematics.

The gauge-invariant Berry curvature, $\Omega_{\mu\nu}$, is defined as the curl of the Berry connection,

$$\Omega_{\mu\nu} = \partial_\mu A_\nu - \partial_\nu A_\mu. \tag{54}$$

Substituting Eq. (51) into this definition yields:

$$\Omega_{\mu\nu} = \partial_\mu(\hat{\Phi}_1^{\mathrm{T}} \mathcal{J}\partial_\nu \hat{\Phi}_1) - \partial_\nu(\hat{\Phi}_1^{\mathrm{T}} \mathcal{J}\partial_\mu \hat{\Phi}_1). \tag{55}$$

Applying the product rule, the terms containing second derivatives $\partial_\mu\partial_\nu\hat{\Phi}_1$ commute and cancel due to the antisymmetry of the expression. We are therefore left with

$$\Omega_{\mu\nu} = (\partial_\mu \hat{\Phi}_1)^{\mathrm{T}} \mathcal{J}(\partial_\nu \hat{\Phi}_1) - (\partial_\nu \hat{\Phi}_1)^{\mathrm{T}} \mathcal{J}(\partial_\mu \hat{\Phi}_1). \tag{56}$$

Because $\mathcal{J}^{\mathrm{T}} = -\mathcal{J}$, the transpose of the second term gives $(\partial_\mu \hat{\Phi}_1)^{\mathrm{T}} \mathcal{J}(\partial_\nu \hat{\Phi}_1)$. Thus, the real Berry curvature takes the elegant form,

$$\Omega_{\mu\nu} = 2(\partial_\mu \hat{\Phi}_1)^{\mathrm{T}} \mathcal{J}(\partial_\nu \hat{\Phi}_1). \tag{57}$$

We can now return to the antisymmetric part of the RQGT in Eq. (48). Working out the term containing the projector P, we find,

$$(\partial_\mu \hat{\Phi}_1)^{\mathrm{T}} \mathcal{J} P(\partial_\nu \hat{\Phi}_1) = (\partial_\mu \hat{\Phi}_1)^{\mathrm{T}} \left(\hat{\Phi}_2 \hat{\Phi}_1^{\mathrm{T}} - \hat{\Phi}_1 \hat{\Phi}_2^{\mathrm{T}} \right) (\partial_\nu \hat{\Phi}_1). \tag{58}$$

Because $\hat{\Phi}_1$ is normalized, its derivative is orthogonal to itself, $\hat{\Phi}_1^{\mathrm{T}}\partial_\nu\hat{\Phi}_1 = 0$. Consequently, both terms in the parenthesis vanish. The projector P drops out of the antisymmetric component, leaving

$$\langle \partial_\mu \hat{\Phi}_1, \mathcal{J}(I_6 - P)\partial_\nu \hat{\Phi}_1 \rangle_{\mathbb{R}} = (\partial_\mu \hat{\Phi}_1)^{\mathrm{T}} \mathcal{J}(\partial_\nu \hat{\Phi}_1) = \frac{1}{2}\Omega_{\mu\nu}. \tag{59}$$

Thus, the Real Quantum Geometric Tensor is compactly expressed as

$$\mathcal{T}_{\mu\nu} = g_{\mu\nu} - \frac{i}{2}\Omega_{\mu\nu}, \tag{60}$$

in exact structural agreement with the complex formalism. This derivation demonstrates that the Fubini-Study metric and the Berry curvature emerge naturally from the real 6D Euclidean geometry of the rotating shallow water equations, driven entirely by the antisymmetric kinematic matrix $\mathcal{J}$.

 doi:10.20944/preprints202605.0606.v1

4. Explicit Matrix and Metric Form of the Fubini-Study Metric

Having formally derived the real geometric tensors, we now explicitly calculate the Fubini-Study metric $g_{\mu\nu}$ for the propagating Poincaré modes in the extended three-dimensional parameter space, $\boldsymbol{p} = (k_x, k_y, f)$. The invariant line element in this space is given by the quadratic form,

$$ds^2 = g_{\mu\nu} dp^\mu dp^\nu. \tag{61}$$

To construct the explicit 3×3 metric tensor, we recall the primary normalized state vector for the positive-frequency Poincaré branch, $\omega_+ = \omega = \sqrt{k^2 + f^2}$,

$$\hat{\Phi}_{P1}(\boldsymbol{p}) = \frac{1}{\sqrt{2}k\omega} \begin{pmatrix} \omega k_x \\ \omega k_y \\ k^2 \\ -f k_y \\ f k_x \\ 0 \end{pmatrix}. \tag{62}$$

The Fubini-Study metric is defined as $g_{\mu\nu} = (\partial_\mu \hat{\Phi}_{P1})^{\mathrm{T}} (I_6 - P)(\partial_\nu \hat{\Phi}_{P1})$. Because the projector $P(\boldsymbol{p}) = \hat{\Phi}_{P1}\hat{\Phi}_{P1}^{\mathrm{T}} + \hat{\Phi}_{P2}\hat{\Phi}_{P2}^{\mathrm{T}}$ removes any variations that merely rotate the state within the degenerate $SO(2)$ subspace, $g_{\mu\nu}$ isolates the true, gauge-invariant changes in the physical state.

To compute the derivatives $\partial_\mu \hat{\Phi}_{P1}$, we apply the chain rule with respect to the coordinates (k_x, k_y, f), keeping in mind that $k = \sqrt{k_x^2 + k_y^2}$ and $\omega = \sqrt{k^2 + f^2}$. For instance, the derivative with respect to f requires $\partial_f \omega = f/\omega$ and $\partial_f k = 0$. Performing these derivatives and projecting them through $(I_6 - P)$ yields a symmetric matrix. After algebraic simplification, the explicit components of the metric tensor are found to be,

$$g_{k_x k_x} = \frac{1}{2k^2\omega^2}\left[\omega^2 - \frac{k_x^2}{k^2}(\omega^2 + f^2)\right] + \frac{k_x^2}{2\omega^4}, \tag{63}$$

$$g_{k_y k_y} = \frac{1}{2k^2\omega^2}\left[\omega^2 - \frac{k_y^2}{k^2}(\omega^2 + f^2)\right] + \frac{k_y^2}{2\omega^4}, \tag{64}$$

$$g_{ff} = \frac{k^2}{2\omega^4}. \tag{65}$$

The off-diagonal terms, representing the cross-sensitivities between parameter variations, are

$$g_{k_x k_y} = g_{k_y k_x} = -\frac{k_x k_y f^2}{k^4 \omega^2} + \frac{k_x k_y}{2\omega^4}, \tag{66}$$

$$g_{k_x f} = g_{f k_x} = -\frac{k_x f}{2\omega^4}, \quad g_{k_y f} = g_{f k_y} = -\frac{k_y f}{2\omega^4}. \tag{67}$$

These components form a real, symmetric 3×3 matrix. Physically, this metric tensor defines a curved Riemannian geometry on the momentum-rotation parameter space. The diverging terms proportional to $1/k^2$ as $k \to 0$ signal the structural boundary where the distinction between longitudinal and transverse propagating waves breaks down, while the well-behaved terms scaled by $1/\omega^4$ guarantee the smooth geometric crossover between rotation-dominated (geostrophic) and gravity-dominated parameter regimes.[2]

[2] We emphasize that our real Stueckelberg formulation maintains the state vectors in the natural, physical basis of the fluid variables (velocity and height). In this physical basis, the horizontal momentum variables (k_x, k_y) are kinematically distinct from the background rotational parameter f. By explicitly defining our real quadrature state $\hat{\Phi}_{P1}$, we have effectively made a specific, global gauge choice that locks the phase of the propagating waves to the horizontal momentum vector, as evident in the $1/k$ normalization factor. As we approach the geostrophic limit at the poles of the parameter sphere where the horizontal momentum vanishes, $k \to 0$, and the frequency is entirely dominated by rotation, $\omega \to f$, our chosen momentum-locked

 doi:10.20944/preprints202605.0606.v1

5. Explicit Antisymmetric 2-Form for the Berry Curvature

We now turn to the symplectic component of our parameter space, governed by the real Berry curvature. As shown in Sec. **??**, the curvature is defined by the antisymmetric 2-form,

$$\Omega_{\mu\nu} = 2(\partial_\mu \hat{\Phi}_{P1})^{\mathrm{T}} \mathcal{J} (\partial_\nu \hat{\Phi}_{P1}). \tag{68}$$

This mathematically translates into an alternating differential form in the three-dimensional space $\boldsymbol{p}$, which can be elegantly mapped to a pseudo-vector field $\boldsymbol{\Omega} = (\Omega_{k_y f}, \Omega_{f k_x}, \Omega_{k_x k_y})$ via the Levi-Civita symbol,

$$\Omega_\lambda = \frac{1}{2} \epsilon_{\mu\nu\lambda} \Omega_{\mu\nu}. \tag{69}$$

Evaluating this requires taking the inner product of the parametric derivatives of the primary state with its Stueckelberg partner, $\hat{\Phi}_{P2} = \mathcal{J} \hat{\Phi}_{P1}$. Let us explicitly calculate the in-plane momentum component, $\Omega_{k_x k_y}$, which represents the accumulation of the classical phase as a wave packet is transported around a closed loop in the (k_x, k_y) momentum space at a fixed latitude f.

Using the derivatives of $\hat{\Phi}_{P1}$ constructed previously, we evaluate the matrix product,

$$\Omega_{k_x k_y} = 2 \left(\frac{\partial \hat{\Phi}_{P1}}{\partial k_x} \right)^{\mathrm{T}} \hat{\Phi}_{P2}^{(k_y)}, \tag{70}$$

where $\hat{\Phi}_{P2}^{(k_y)}$ denotes the partial derivative of the second quadrature state with respect to k_y. After expanding the six-dimensional dot product, cross-canceling symmetric terms, and factoring the polynomial expressions using $k^2 = \omega^2 - f^2$, the algebraic reduction yields a nice compact expression,

$$\Omega_{k_x k_y} = \frac{2f}{\omega^3} = \frac{2f}{(k_x^2 + k_y^2 + f^2)^{3/2}}. \tag{71}$$

Applying the identical procedure to the remaining orthogonal parameter planes, (k_y, f) and (f, k_x), we find the remaining components of the antisymmetric tensor. Because the physical system is isotropic in the horizontal momentum plane, the derivation is structurally symmetric, yielding

$$\Omega_{k_y f} = \frac{2k_x}{\omega^3}, \quad \Omega_{f k_x} = \frac{2k_y}{\omega^3}. \tag{72}$$

Assembling these components, the total real Berry curvature 2-form can be expressed as a dual vector field in the extended parameter space,

$$\boldsymbol{\Omega}(\boldsymbol{p}) = \frac{2\boldsymbol{p}}{|\boldsymbol{p}|^3}. \tag{73}$$

Thus, the antisymmetric geometry of our real Stueckelberg state vectors naturally led to the exact expression for a topological magnetic monopole situated at the origin of the parameter space, $(k_x = 0, k_y = 0, f = 0)$. Unlike traditional complex formulations where such monopoles arise from the abstract geometry of Hermitian matrices, here the monopole emerges purely from the classical kinematic rotation matrix $\mathcal{J}$ acting on the fluid's Euclidean energy metric. The topological charge of this monopole is $C = 2$, corresponding to the number of topologically protected edge states (Kelvin modes) that must traverse the band gap when the physical fluid domain is bounded.

coordinate frame twists infinitely fast and becomes ill-defined. The geometrically diverging $1/k^2$ terms in our Fubini-Study metric are not physical singularities, but rather coordinate singularities. They represent the Riemannian penalty for utilizing a global coordinate grid that pinches at the poles. In the complex Spin-1 formalism, this is analogous to the Dirac string singularity, which is elegantly masked by the complex projective geometry but inevitably manifests when one attempts to construct a single, globally smooth real basis for the wavefunctions.

 doi:10.20944/preprints202605.0606.v1

6. Scale Invariance and the Null Subspace of the Metric

As was pointed out in Ref. [10], despite the apparent algebraic complexity of the real Fubini-Study metric in Cartesian coordinates, its underlying geometric structure contains a notable simplification: the 3×3 metric tensor possesses a one-dimensional null subspace. This null subspace reflects the fundamental scale invariance of the classical fluid equations.

By inspecting the normalized primary state vector $\hat{\Phi}_{P1}$, we notice that every non-zero component is a homogeneous function of degree zero with respect to the parameters. Specifically, the numerator of each component carries a combined polynomial degree of 2 in the variables (k_x, k_y, f), which is balanced by the denominator $k\omega$. Consequently, if we scale the entire parameter vector by an arbitrary positive constant λ, such that $(k_x, k_y, f) \to (\lambda k_x, \lambda k_y, \lambda f)$, the fluid frequency scales linearly as $\omega \to \lambda\omega$, but the state vector $\hat{\Phi}_{P1}$ remains entirely unchanged. Physically, this means that moving radially outward from the origin in the parameter space increases the energy of the wave, but it preserves the fundamental physical structure (the relative amplitudes and phase differences) of the fluid mode. Because the physical state does not vary along this radial direction, the derivative of the state projected along the radial parameter vector $\boldsymbol{p} = (k_x, k_y, f)^{\mathrm{T}}$ must vanish,

$$p^{\mu}\partial_{\mu}\hat{\Phi}_{P1} = k_x \frac{\partial \hat{\Phi}_{P1}}{\partial k_x} + k_y \frac{\partial \hat{\Phi}_{P1}}{\partial k_y} + f \frac{\partial \hat{\Phi}_{P1}}{\partial f} = 0. \tag{74}$$

It immediately follows that contracting the metric tensor with this radial vector yields zero,

$$g_{\mu\nu}p^{\nu} = 0. \tag{75}$$

Thus, the vector $\boldsymbol{p}$ spans the one-dimensional null subspace of the metric.

To explicitly isolate this null subspace and diagonalize the metric with respect to the radial direction, we can perform a coordinate transformation from the Cartesian parameters (k_x, k_y, f) to spherical parameters (p, θ, ϕ), where the radial coordinate is defined directly by the wave frequency,

$$p = \sqrt{k_x^2 + k_y^2 + f^2} = \omega. \tag{76}$$

In this spherical basis, the radial geometric variations are governed by the partial derivative $\partial/\partial p$. Because the state vectors are independent of the radial magnitude p, all p-derivatives vanish. Consequently, in the spherical parameter basis, the transformed Fubini-Study metric $\tilde{g}_{ab}$ assumes a block-diagonal form with an explicit zero on the diagonal (cf. [10]),

$$\tilde{g}_{ab} = \begin{pmatrix} 0 & 0 & 0 \\ 0 & g_{\theta\theta} & g_{\theta\phi} \\ 0 & g_{\phi\theta} & g_{\phi\phi} \end{pmatrix}. \tag{77}$$

This transformed metric clarifies the geometry of the system. It demonstrates that all true, invariant geometric variations of the fluid modes reside exclusively on the two-dimensional surface of the parameter sphere parameterized by the angles θ and ϕ. The radial direction simply acts as a trivial, null gauge direction, reinforcing that the topological invariant (the monopole) is entirely determined by the angular winding of the real fluid state.

7. The Archean Earth as a Topological Phase Transition

In condensed matter systems the control parameters of a topological Hamiltonian can be tuned explicitly via external magnetic fields or strain. In our real rotating fluid formulation, the background rotation f acts as the analogous macroscopic dial. While we cannot physically alter the rotation rate of the modern Earth to experimentally verify the geometric sensitivities encoded in our Fubini-Study metric, the geological history of the planet has already performed this experiment over deep time.

 doi:10.20944/preprints202605.0606.v1

During the Archean eon, approximately three to four billion years ago, the Earth rotated significantly faster, with a day lasting approximately 14 hours. The global Coriolis parameter f was correspondingly larger. To understand the topological consequence of this ancient regime, we rely on the principle of dynamic similarity, governed by the fundamental length scale of rotating shallow water theory: the Rossby radius of deformation, L_R,

$$L_R = \frac{\sqrt{gH}}{f}, \tag{78}$$

where, we recall, g is gravity and H is the equivalent fluid depth.

The Rossby radius characterizes the spatial extent of rotationally trapped fluid structures, including topologically protected boundary modes such as equatorial Kelvin waves. Because L_R is inversely proportional to f, the primordial Earth possessed a dramatically smaller Rossby radius. From the perspective of the fluid's parameter space, the ancient oceans "felt" topologically vaster. The energy gap separating the low-frequency geostrophic modes from the high-frequency propagating Poincaré modes, which is proportional to f at the origin of momentum space, was significantly wider.

Planetary weather systems and ocean eddies in the Archean regime would have been tightly confined, creating highly fragmented, narrow zonal jets. The topologically protected edge modes would have been compressed against boundaries or the equator. Over billions of years, tidal friction generated by the moon has acted as a slow, planetary-scale dial, steadily decreasing f. This gradual tidal braking has effectively swept the Earth's oceans and atmosphere through a continuous topological phase transition, lowering the band gap, expanding the Rossby radius, and shifting the fluid modes through the geometric curvatures described by our real Fubini-Study metric.

While the fossil record does not preserve high-frequency fluid dynamics, the rigorous scaling laws of our real geometric formulation guarantee that this planetary evolution can be replicated at the laboratory scale. Correspondingly, we propose a macroscopic Geophysical Fluid Dynamics (GFD) laboratory experiment designed to directly observe this topological phase transition and explicitly measure the geometric tensors derived in Sec. 4 and 5. By utilizing a rotating fluid tank, we can construct a "fast-forward time machine" that compresses billions of years of planetary tidal braking into a controlled experimental sweep.

The experimental setup consists of a parabolic rotating tank filled with a shallow layer of fluid, mounted on a motorized turntable. The motor serves as the precise external dial for the parameter f. To replicate the conditions of the Archean oceans, the tank is initially spun up to a high angular velocity $\Omega_{\max}$, establishing a wide topological band gap. An oscillating paddle or pneumatic wavemaker positioned at the radial boundary is used to continuously inject a broad spectrum of wave energy into the system. Particle Image Velocimetry (PIV) would then be deployed to capture the real, high-resolution Eulerian velocity field $\boldsymbol{u}(x, y, t)$ and the free surface elevation $\eta(x, y, t)$ via laser sheet illumination and fluorescent tracer particles. This would provide direct empirical access to the physical, six-dimensional real Stueckelberg state vectors $\hat{\Phi}$ at every point in the basin. The corresponding experimental procedure would operate as follows:

1. **Steady State Initialization:** The system is driven at high f to establish the Archean regime. The PIV measurements will verify the tight spatial confinement of the boundary modes (Kelvin waves) and the wide spectral gap between geostrophic eddies and bulk Poincaré waves.
2. **The Parameter Sweep:** The turntable is decelerated, acting as an artificial tidal brake. This sweeps the control parameter f downward toward the modern Earth regime and ultimately toward $f = 0$ (the non-rotating topological degeneracy point).
3. **Extracting the Geometry:** During the spin-down, the real-time PIV data is Fourier-transformed to track the evolution of the fluid eigenmodes in momentum space. By measuring the changing inner products of the physical state vectors as f decreases, we can directly compute the real parametric derivatives $\partial_f \hat{\Phi}$.

 doi:10.20944/preprints202605.0606.v1

This approach allows for the empirical reconstruction of the g_{ff} and cross-term $g_{k_x f}$ components of the Fubini-Study metric. As $f \to 0$, the experiment will directly capture the closing of the energy gap, the macroscopic spatial widening of the boundary modes, and the divergent geometric sensitivity predicted by the metric. By mapping real fluid variables to real geometric tensors, this table-top analog will physically validate the Stueckelberg parameter space geometry without relying on complex abstract spaces.

8. Unbroken Supersymmetry in the Real Stueckelberg Formulation

An interesting consequence of mapping the classical rotating shallow water equations into the real Stueckelberg Hilbert space is that the system naturally admits an exact, unbroken supersymmetric interpretation. In our 6D real formalism, the supersymmetric algebra emerges directly from the kinematics of the classical fluid.

In Witten's formulation of supersymmetric quantum mechanics, the defining characteristic of a SUSY system is the existence of a self-adjoint supercharge operator, $\mathcal{Q}$, from which the system's energy Hamiltonian, $\mathcal{H}_{\text{SUSY}}$, is generated via its square,

$$\mathcal{H}_{\text{SUSY}} = \mathcal{Q}^2. \tag{79}$$

Within our real six-dimensional approach, the symmetric Stueckelberg Hamiltonian derived in Sec. 2.2 fulfills the role of the fundamental supercharge,

$$\mathcal{Q} \equiv \mathcal{H}_S = \begin{pmatrix} -K & F \\ -F & -K \end{pmatrix} = \begin{pmatrix} 0 & 0 & k_x & 0 & f & 0 \\ 0 & 0 & k_y & -f & 0 & 0 \\ k_x & k_y & 0 & 0 & 0 & 0 \\ 0 & -f & 0 & 0 & 0 & k_x \\ f & 0 & 0 & 0 & 0 & k_y \\ 0 & 0 & 0 & k_x & k_y & 0 \end{pmatrix}. \tag{80}$$

Because $\mathcal{H}_S$ is purely real and symmetric, its square generates a positive semi-definite, real symmetric operator. We therefore define the true Supersymmetric Hamiltonian of the fluid as

$$\mathcal{H}_{\text{SUSY}} = \mathcal{H}_S^2 = \begin{pmatrix} k_x^2 + f^2 & k_x k_y & 0 & 0 & 0 & f k_y \\ k_x k_y & k_y^2 + f^2 & 0 & 0 & 0 & -f k_x \\ 0 & 0 & k^2 & -f k_y & f k_x & 0 \\ 0 & 0 & -f k_y & k_x^2 + f^2 & k_x k_y & 0 \\ 0 & 0 & f k_x & k_x k_y & k_y^2 + f^2 & 0 \\ f k_y & -f k_x & 0 & 0 & 0 & k^2 \end{pmatrix}. \tag{81}$$

By acting with this operator on our basis states, we obtain the eigenvalue equation,

$$\mathcal{H}_{\text{SUSY}} \Phi = \omega^2 \Phi. \tag{82}$$

The eigenvalues of this SUSY Hamiltonian are the squared frequencies of the physical fluid waves, perfectly aligning with the non-negative energy spectrum required by supersymmetry, $E \geq 0$.

The physical importance of this identification lies in the classification of the fluid's spectrum. In SUSY theory, a supersymmetry is considered "unbroken" if and only if there exists a ground state vacuum, $|0\rangle$, that is annihilated by the supercharge, resulting in the zero energy,

$$\mathcal{Q}|0\rangle = 0 \implies E = 0. \tag{83}$$

 doi:10.20944/preprints202605.0606.v1

For our planetary fluid system, we apply the real supercharge to the geostrophic zero-modes derived in Sec. 2.3,

$$\mathcal{Q}\hat{\Phi}_{G1} = 0, \quad \mathcal{Q}\hat{\Phi}_{G2} = 0. \tag{84}$$

This reveals a physically interesting correspondence: the classical steady-state geostrophic balance—the fundamental mechanism driving large-scale weather patterns and ocean currents—is mathematically identical to the unbroken supersymmetric vacuum of the parameter space. The topological zero-modes are precisely the unbroken SUSY ground states.

Furthermore, supersymmetry demands that all excited states with $E > 0$ must consist of degenerate pairs, formally identified as bosonic and fermionic superpartners, which are transformed into one another by the action of the supercharge $\mathcal{Q}$. Specifically, at $f = 0$, the bosonic superpartner (pure potential energy) consists entirely of the scalar height anomaly,

$$\hat{\Phi}_B = \begin{pmatrix} 0 \\ 0 \\ 1 \\ 0 \\ 0 \\ 0 \end{pmatrix}, \tag{85}$$

while the fermionic superpartner (pure kinetic energy) consists entirely of the vector velocity field,

$$\hat{\Phi}_F = \frac{1}{k} \begin{pmatrix} -k_x \\ -k_y \\ 0 \\ 0 \\ 0 \\ 0 \end{pmatrix}, \tag{86}$$

with the two states transforming into each other under the action of $\mathcal{Q}$,

$$\mathcal{Q}\hat{\Phi}_B = \omega\hat{\Phi}_F, \quad \mathcal{Q}\hat{\Phi}_F = \omega\hat{\Phi}_B. \tag{87}$$

In our fluid system, these excited states correspond to the propagating Poincaré modes, which possess strictly positive SUSY energy, $E = \omega^2 = k^2 > 0$.

It is important to emphasize that in our real formulation, at $f \neq 0$, the physical wave itself represents this excited SUSY multiplet. Because the supercharge contains spatial gradients, K, it intrinsically couples the scalar height anomalies to the horizontal velocities. Thus, a propagating gravity wave is a hybridized state consisting of both a bosonic sector (the potential energy of the height field) and a fermionic sector (the kinetic energy of the velocity field), naturally satisfying the superpartner requirement of Witten's algebra.

Separately, the system also possesses a twofold kinematic degeneracy guaranteed by the antisymmetric complex structure operator $\mathcal{J}$. Because the generator of the dynamics $\mathcal{G}$ commutes with $\mathcal{J}$, our supercharge also commutes with the complex structure, $[\mathcal{Q}, \mathcal{J}] = 0$. Consequently, if $\hat{\Phi}_{P1}$ is a propagating eigenmode of $\mathcal{Q}$, its Stueckelberg partner $\hat{\Phi}_{P2} = \mathcal{J}\hat{\Phi}_{P1}$ is guaranteed to be an orthogonal eigenstate with the same eigenvalue. This simply reflects the $SO(2)$ rotational gauge freedom between the sine and cosine quadratures of the physical wave.

Thus, the rotating shallow water system is mapped onto an unbroken supersymmetric quantum mechanics entirely within $\mathbb{R}^6$, whose algebra is given by,

$$[\mathcal{Q}, \mathcal{J}] = 0, \quad [\mathcal{H}_{\text{SUSY}}, \mathcal{J}] = 0. \tag{88}$$

 doi:10.20944/preprints202605.0606.v1

The geostrophic weather patterns serve as the zero-energy SUSY vacuum, while the propagating gravity waves form the excited supermultiplets.

To complete the supersymmetric classification of our fluid system, we must establish a mathematical mechanism to distinguish between the superpartners. In standard SUSY QM, this is achieved by defining a chiral grading operator, commonly denoted as Γ (the analog of the parity operator $(-1)^F$ or the Dirac γ_5 matrix). This operator partitions the Hilbert space into two distinct sectors: a "bosonic" sector with eigenvalue $+1$, and a "fermionic" sector with eigenvalue -1.

In our real Stueckelberg parameter space, the physical nature of the state variables provides a remarkably intuitive geometric grading. The state vector is composed of two physically distinct types of fields: the scalar fluid height deviation η (which is isotropic and relates to potential energy) and the vector velocity components u and v (which are directional and relate to kinetic energy). We can formally define the scalar height fields as the bosonic sector, and the vector velocity fields as the fermionic sector.

Operating within the 6×6 real Hilbert space defined by the basis $(u_1, v_1, \eta_1, u_2, v_2, \eta_2)^{\mathrm{T}}$, the corresponding chiral grading matrix is defined as a diagonal involution,

$$\Gamma = \begin{pmatrix} -1 & 0 & 0 & 0 & 0 & 0 \\ 0 & -1 & 0 & 0 & 0 & 0 \\ 0 & 0 & 1 & 0 & 0 & 0 \\ 0 & 0 & 0 & -1 & 0 & 0 \\ 0 & 0 & 0 & 0 & -1 & 0 \\ 0 & 0 & 0 & 0 & 0 & 1 \end{pmatrix}. \tag{89}$$

By construction, Γ is real, symmetric, $\Gamma^{\mathrm{T}} = \Gamma$, and its square is the identity, $\Gamma^2 = I_6$.[3]

In a purely non-rotating fluid system, $f = 0$, calculating the anticommutator of the grading operator with the supercharge reveals an exact chiral symmetry,

$$\{\Gamma, \mathcal{Q}\}_{f=0} = (\Gamma\mathcal{Q} + \mathcal{Q}\Gamma)_{f=0} = 0, \quad [\Gamma, \mathcal{H}_{\mathrm{SUSY}}]_{f=0} = 0. \tag{90}$$

The anticommutation relation guarantees that for every state Φ with energy E, the state $\Gamma\Phi$ has energy $-E$. Because $\mathcal{Q}^2$ gives the physical energy squared, this enforces that all non-zero energy modes (the propagating gravity waves) must exist in symmetric pairs.

When planetary rotation is introduced, $f \neq 0$, the Coriolis force fundamentally alters this structure. Looking at the block-off-diagonal position of the matrix F within the supercharge $\mathcal{Q}$, the rotation parameter f acts as an explicit coupling between the orthogonal velocity components u and v *across* the distinct Stueckelberg phase blocks. For instance, it couples the cosine-quadrature velocity u_1 in the upper block to the sine-quadrature velocity v_2 in the lower block.[4]

[3] While the designation of macroscopic fluid variables as "bosons" or "fermions" is an analogy borrowed from quantum mechanics, the mathematical structure of the grading operator Γ is inherent to the fluid's kinematics. Geometrically speaking, it encodes spatial parity: the scalar height anomaly η is even under spatial inversion, acting as a bosonic scalar field, while the directional velocity components u and v are odd, acting as fermionic vector fields. From the algebraic standpoint, Γ formalizes the bipartite interaction nature of the pressure-gradient forces at $f = 0$, where the time evolution of the scalar field depends exclusively on the vector fields, and vice versa (the variables are locked in a "checkerboard" pattern where height only talks to velocity, and velocity only talks to height.

[4] This makes good physical sense. The Coriolis acceleration is proportional to velocity, $\partial_t u \propto fv$. Taking a time derivative shifts a cosine wave into a sine wave. Therefore, the Coriolis force acts as a cross-quadrature, fermion-fermion interaction.

 doi:10.20944/preprints202605.0606.v1

In our supersymmetric lexicon, this constitutes a pure cross-quadrature fermion-fermion interaction. Because this Coriolis term links fermions to fermions, it does not flip sign under conjugation by Γ, causing the exact chiral anticommutation to be broken,

$$\{\Gamma, \mathcal{Q}\} = \begin{pmatrix} 0 & 0 & 0 & 0 & -2f & 0 \\ 0 & 0 & 0 & 2f & 0 & 0 \\ 0 & 0 & 0 & 0 & 0 & 0 \\ 0 & 2f & 0 & 0 & 0 & 0 \\ -2f & 0 & 0 & 0 & 0 & 0 \\ 0 & 0 & 0 & 0 & 0 & 0 \end{pmatrix} \neq 0,$$
$$[\Gamma, \mathcal{H}_{\text{SUSY}}] = 2f\Sigma \neq 0, \quad \Sigma \equiv \begin{pmatrix} 0 & 0 & 0 & 0 & 0 & -k_y \\ 0 & 0 & 0 & 0 & 0 & k_x \\ 0 & 0 & 0 & -k_y & k_x & 0 \\ 0 & 0 & k_y & 0 & 0 & 0 \\ 0 & 0 & -k_x & 0 & 0 & 0 \\ k_y & -k_x & 0 & 0 & 0 & 0 \end{pmatrix}. \tag{91}$$

This behaves analogously to a chiral-symmetry-breaking mass term in the Dirac equation. Importantly, however, while the strict chiral symmetry is broken by the planet's rotation, the fundamental unbroken supersymmetry of the Hamiltonian, $\mathcal{H}_{\text{SUSY}} = \mathcal{Q}^2$, remains intact.[5]

The utility of this grading lies in the calculation of the Witten Index, W, a topological invariant that counts the difference between the number of bosonic (n_B) and fermionic (n_F) zero-energy ground states. The index is defined as the trace of the grading operator over the entire Hilbert space,

$$W = \text{Tr}(\Gamma) = n_B - n_F. \tag{92}$$

Taking the trace of our explicit 6×6 grading matrix yields

$$W = -2. \tag{93}$$

This simple integer result is important. A fundamental theorem of supersymmetric quantum mechanics states that if $W \neq 0$, the supersymmetry cannot be dynamically broken. The non-vanishing index topologically guarantees the existence of at least $|W|$ zero-energy ground states.

In our 6D system, $|W| = 2$ predicts the existence of exactly two unbroken zero-modes. These are precisely the two real dimensions of the geostrophic branch ($\hat{\Phi}_{G1}$ and $\hat{\Phi}_{G2}$) derived in Sec. 2.3. Thus, we arrive at a striking topological conclusion: the permanent existence of large-scale steady-state geostrophic weather patterns on a rotating planet is topologically protected by the non-zero Witten index of the classical fluid's kinematics.

It is instructive to contrast this supersymmetric classification with the foundational topological characterization introduced by Delplace *et al.* [3]. In their approach, the topological invariants of the fluid are identified by calculating the Chern numbers of the complexified energy bands. This process requires integrating the Berry curvature over the entire parameter space manifold to predict the emergence of propagating edge modes (Kelvin and Yanai waves) via the bulk-boundary correspondence.

In contrast, our calculation of the Witten index $W = -2$ is derived purely algebraically from the chiral grading of the real physical variables, without the need for global integration over a complexified bundle. While the Chern number characterizes the global geometric twisting of the excited, propagating Poincaré bands, the Witten index acts as a spectral invariant that directly counts the unbroken zero-

[5] To put it simply, even though f ruins the perfect anti-commutation of Γ and Q, it does not destroy the $E = 0$ vacuum. That is, while the Coriolis force makes the wave mixing messier, it cannot lift the geostrophic weather modes off of the zero energy!

 doi:10.20944/preprints202605.0606.v1

energy geostrophic modes. Together, these two distinct topological invariants provide a complete, complementary picture of the shallow water system: the Chern number of Delplace *et al.* controls the topologically protected high-frequency edge states, whereas our real Witten index topologically protects the permanent existence of the low-frequency geostrophic bulk states.

9. Resolution of the Real Wave and Mode Selection Ambiguities

While the topological origin of equatorial waves was established by Delplace *et al.* [3], their reliance on a complexified pseudo-spin mapping left critical conceptual vulnerabilities in the theory. These vulnerabilities were prominently highlighted in a commentary by Biello and Dimofte [11], who raised two primary concerns regarding the application of quantum topological methods to classical fluids. First, they noted that quantum winding numbers naturally arise from the rotating phase of complex-valued wave functions; therefore, if classical physical waves are real-valued linear combinations of these complex states, it must be explained why the topological winding numbers do not simply cancel out through destructive interference. Second, they pointed out that quantum electron systems rely on a rigorously defined Fermi sea at zero temperature to unambiguously determine the ground state, thereby fixing the chirality of edge states. Because classical fluids lack a Pauli exclusion principle or a Fermi sea, arbitrary pairings of bulk modes across the equator could theoretically predict both eastward and westward equatorial modes. A complete topological theory must provide a rigorous mechanism that favors the observed eastward propagation of Kelvin waves.

The real Stueckelberg six-dimensional formalism, combined with the unbroken supersymmetric vacuum derived in the previous section, may resolve both of these ambiguities.

Regarding the first concern (the supposed cancellation of real topological winding) our derivation demonstrates that the Berry curvature in classical fluids is not an artifact of a complex quantum phase. By separating the complex quantum geometric tensor into its real Fubini-Study metric $g_{\mu\nu}$ and its real Berry curvature $\Omega_{\mu\nu}$, we showed that the curvature is fundamentally a symplectic geometric form. The rotational "phase" is generated purely by the real, antisymmetric super-selection operator $\mathcal{J}$, which enforces a classical $SO(2)$ kinematic rotation between the orthogonal sine and cosine quadratures of the wave. Because the macroscopic states $\hat{\Phi}_1$ and $\hat{\Phi}_2 = \mathcal{J}\hat{\Phi}_1$ act as independent orthogonal basis vectors in the $\mathbb{R}^6$ space, their wedge products do not cancel upon superposition. Instead, together they define a real oriented area in the parameter space. The topological monopole charge of $C = 2$ is therefore an invariant property of the fluid's real symplectic kinematics, requiring no imaginary phase to survive.

Regarding the second concern (the lack of a Fermi sea to govern the eastward vs. westward mode selection) our mapping to supersymmetric quantum mechanics provides the required physical anchor. In a standard quantum approach, one might attempt to define raising and lowering ladder operators to traverse the energy bands. However, in our unbroken SUSY fluid formulation, the effective spectrum is defined by $E = \omega^2 = k^2 + f^2$. This yields highly degenerate positive-energy superpartners containing both the forward-propagating Poincaré modes (the P branch, $\omega > 0$) and the reverse-propagating modes (the N branch, $\omega < 0$).

Notice that the system does not require a continuous ladder operator to bridge these excited modes to the geostrophic states. Instead, the fluid is governed by an isolated zero-energy vacuum sector with $E = 0$, mathematically protected by a non-zero Witten index of $W = -2$. This unbroken supersymmetric vacuum replaces the role of the quantum Fermi sea. In classical fluid dynamics, these zero-energy modes correspond to the conservation of potential vorticity (PV). Because the geostrophic vacuum is topologically isolated from the propagating bands by the Coriolis parameter f, the bulk-boundary correspondence is rigorously constrained.

When the rotation parameter f smoothly changes sign across the planetary equator, the spectral flow of the system must bridge the gap between the excited Poincaré bands and the protected $W = -2$ vacuum. While the forward, P, and reverse, N, propagating bulk modes share the same squared SUSY energy E, they belong to orthogonal superselection sectors defined by their physical frequency ω.

 doi:10.20944/preprints202605.0606.v1

Time-reversal symmetry is explicitly broken by the planetary rotation f. Consequently, the integration of the real Berry curvature over the positive-frequency sub-manifold specifies the spectral winding direction. Because the fluid must connect the positive-frequency bulk band to the uniquely defined zero-energy PV vacuum as $f \to -f$, the topology selects edge modes with a positive group velocity. The arbitrary pairing of northern and southern bulk states is physically prohibited by the isolation of the Witten index, thereby mathematically guaranteeing the eastward propagation of the equatorial Kelvin waves without invoking an artificial electron Fermi sea.

10. Conclusions

In this paper, we have demonstrated that the rich topological phenomena inherent to planetary fluid dynamics do not require the invocation of complex numbers or abstract Hamiltonians. By mapping the classical rotating shallow water equations into a real, six-dimensional Stueckelberg Hilbert space, we have shown that the topological band structure of planetary waves is an intrinsic property of the fluid's kinematics in $\mathbb{R}^6$.

Through this inherently real formulation, we decoupled the conventional complex Quantum Geometric Tensor into its fundamental geometric constituents. We established that the Fubini-Study metric and the Berry curvature must be viewed as independent, real geometric objects. This approach explicitly revealed the emergence of a topological magnetic monopole of charge $C = 2$ purely from the real antisymmetric rotational kinematics of the classical wave quadratures. Furthermore, by retaining the state vectors in the physical basis of fluid variables (velocity and height), our real Fubini-Study metric explicitly captured the scale-invariance of the fluid via a one-dimensional null subspace, while accurately reflecting the coordinate singularities mathematically analogous to the Dirac string.

To physically ground these abstract geometric notions, we proposed a direct connection between the parameter space structure and macroscopic geophysical phenomena. By leveraging the dynamic similarity controlled by the Rossby radius of deformation, we proposed that the variation of the Coriolis parameter f can model the deep-time planetary evolution of the Archean Earth. We translated this planetary-scale topological phase transition into a practical experimental proposal utilizing rotating laboratory tanks, providing a tabletop mechanism to directly measure the real parametric derivatives and geometric tensors of the fluid space.

Finally, we put forward an equivalence between classical geophysical fluid dynamics and supersymmetric quantum mechanics. By identifying the symmetric Stueckelberg Hamiltonian as a purely real supercharge, we showed that the classical rotating shallow water system realizes an unbroken supersymmetric algebra. Through the construction of a real chiral grading matrix, we calculated a fluid Witten index of $W = -2$. This mathematically guarantees the existence of two unbroken, zero-energy ground states, proving that the permanent existence of large-scale, geostrophic weather patterns on a rotating planet is a topologically protected consequence of unbroken supersymmetry.

Ultimately, this real geometric and supersymmetric approach provides a powerful new lens for analyzing classical topological systems. It solidifies the principle that the deep insights of topological band theory and high-energy physics are not exclusive to complex quantum mechanics, but are fundamentally woven into the macroscopic, classical motions of our oceans and atmosphere.

Acknowledgments: The author thanks Alan Dorsey for introducing him to the fascinating topic of topological fluid dynamics.

Appendix A. The Geophysical Waves and Their Topological Origins

This Appendix re-derives the physical waves present in the rotating shallow water model on the basis of the Stueckelberg formalism. It also explains how these waves fit into the broader story of topological physics discussed in this paper.

To understand how topology applies to oceans and atmospheres, it is helpful to look at the fluid in two distinct regions: the open ocean (the bulk) and the equator (the boundary).

 doi:10.20944/preprints202605.0606.v1

Appendix A.1. The Bulk: The Open Ocean and the Frequency Gap

When analyzing a localized region of the ocean far from the equator, the Earth's rotation provides a roughly constant Coriolis parameter, f. In the equations of motion, this rotation acts similarly to a mass term in the Dirac equation. It breaks time-reversal symmetry and creates a frequency gap between different types of fluid motion.

In this bulk region, we find two primary categories of flow:

1. **Poincaré Waves (Inertio-Gravity Waves):** These are relatively high-frequency gravity waves, much like the ripples created by dropping a stone into a pond, but their trajectories are curved by the planet's rotation. They have a dispersion relation of $\omega_{\pm}(\boldsymbol{k}) = \pm\omega$, where $\omega = \sqrt{k^2 + f^2}$. In our 6d formalism, this wave has the form,

$$\hat{\Phi}_{P1}(\boldsymbol{k}) = \frac{1}{\sqrt{2}k\omega} \begin{pmatrix} \omega k_x \\ \omega k_y \\ k^2 \\ -f k_y \\ f k_x \\ 0 \end{pmatrix}, \tag{A1}$$

which encapsulates both the velocity components and the height anomaly, preserving the orthogonal rotational quadratures in the lower block. In the language of topological band theory, these waves form the excited energy bands of the fluid. The geometric properties of these specific waves, such as their Berry curvature and topological monopole charge, are the primary subjects of recent quantum geometric studies, including the recent work by Ganeshan and Dorsey [10], as well as the derivations in the main text of this paper.

2. **Geostrophic Zero-Modes:** These are the slow, large-scale, stationary flow patterns, such as major ocean currents or atmospheric jet streams. They sit at a frequency of $\omega_0(\boldsymbol{k}) = 0$ and are characterized by the conservation of potential vorticity. In our 6d formalism, this wave has the form,

$$\hat{\Phi}_{G1}(\boldsymbol{k}) = \frac{1}{\sqrt{k^2 + f^2}} \begin{pmatrix} 0 \\ 0 \\ f \\ k_y \\ -k_x \\ 0 \end{pmatrix}, \tag{A2}$$

which demonstrates that these stationary modes possess zero divergence and correspond to the geostrophic balance condition. In the supersymmetric formulation discussed in this manuscript, these steady flows serve as the stable ground state, or vacuum, of the system.

Appendix A.2. The Boundary: The Equator as a Domain Wall

Because the Earth is a sphere, the Coriolis parameter f is not uniform. It is largest at the poles, approaches zero at the equator, and changes sign between the Northern and Southern Hemispheres. A common approximation near the equator is

$$f \approx \beta y, \tag{A3}$$

where y is the North-South coordinate. This Coriolis parameter breaks translational symmetry in the North-South direction. We no longer have a plane wave in y; we only have a 1D plane wave traveling in x, so the physical 3D wave takes the form,

$$\Psi(x, y, t) = \Psi_1(y, k_x)\cos(k_x x - \omega t) + \Psi_2(y, k_x)\sin(k_x x - \omega t). \tag{A4}$$

 doi:10.20944/preprints202605.0606.v1

Because y now defines the shape of the bound spatial profile rather than a Fourier momentum variable, those y-dependent profiles act as the amplitudes for the 1D wave. When we stack these quadratures into our Stueckelberg formalism, the 6D state $\Psi(y, k_x) = (\Psi_1^{\mathrm{T}}, \Psi_2^{\mathrm{T}})^{\mathrm{T}}$ naturally retains a y-dependence, becoming the position-dependent amplitude vector in the 6D representation.

In topological physics, when a mass-like parameter such as f changes sign across a spatial line, that line acts as a domain wall. A core principle called the bulk-boundary correspondence states that if the bulk waves (the Poincaré waves) possess a non-trivial topological structure, gapless edge states must emerge along the domain wall. These edge states are required to bridge the frequency gap between the high-frequency bulk bands and the zero-frequency ground state.

Appendix A.3. The Equatorial Waves: Matsuno's Solutions

Long before topological band theory was formulated, Taroh Matsuno [6] (1966) solved the shallow water equations near the equator and cataloged the waves that are naturally trapped there. Because the equator traps these waves, their amplitude decays as one moves further North or South. Three prominent equatorial waves emerged from his analysis (see Fig. A1):

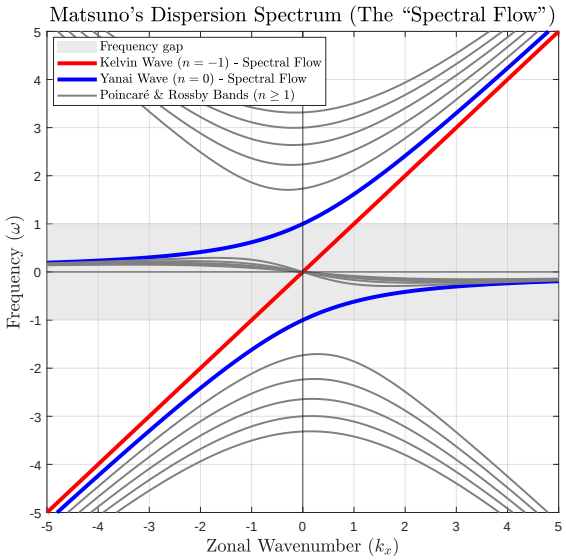

Figure A1. Matsuno's dispersion spectrum illustrating the topological spectral flow of equatorial waves. The gray contours represent the standard bulk modes ($n \geq 1$), which separate into high-frequency Poincaré gravity waves and low-frequency Rossby waves. The light gray region denotes the forbidden frequency gap where bulk modes cannot exist. As required by the low-frequency limit, $-k_x/\omega \approx 2n + 1 + k_x^2$, of the dispersion relation, Eq. (A26), the Rossby bands for $\omega > 0$ occupy the negative k_x domain, enforcing their westward propagation. The Kelvin ($n = -1$, red) and Yanai ($n = 0$, blue) modes exhibit continuous spectral flow, acting as boundary states that bridge the frequency gap and connect the isolated bulk bands across the momentum space.

1. **The Equatorial Kelvin Wave:** This is a boundary wave that travels parallel to the equator with no North-South fluid velocity. It travels only in the eastward direction, and its frequency is proportional to its wavenumber, $\omega = k_x$. With a spatial envelope bounded by the equator,

$$E_0(y) = e^{-\beta y^2/2}, \tag{A5}$$

and an eastward dispersion,

$$\omega = k_x, \tag{A6}$$

 doi:10.20944/preprints202605.0606.v1

the 6d quadrature state for this wave takes the form,

$$\Phi_{\text{Kelvin}}(y, k_x) = E_0(y) \begin{pmatrix} 1 \\ 0 \\ 1 \\ 0 \\ 0 \\ 0 \end{pmatrix}. \tag{A7}$$

This sparse vector explicitly visualizes how the Kelvin wave possesses zero meridional velocity, $v = 0$, and maintains perfectly synchronized zonal velocity and height anomalies, $u = \eta$. Topologically, this wave acts as a chiral edge state that connects the geostrophic zero-modes to the high-frequency Poincaré bands.

2. **The Yanai Wave (Mixed Rossby-Gravity Wave):** This wave exhibits hybrid behavior. At high frequencies, it acts like an eastward-moving gravity wave, while at low frequencies, it acts like a westward-moving Rossby wave. Like the Kelvin wave, it also helps bridge the frequency gap. Representing a mixed hybrid state, the Yanai wave combines the lowest-order Gaussian envelope $E_0(y)$ with the first-order Hermite polynomial spatial mode,

$$E_1(y) \propto y e^{-\beta y^2/2}. \tag{A8}$$

The 6d quadrature state for this wave takes the form,

$$\Phi_{\text{Yanai}}(y, k_x) \propto \begin{pmatrix} u_{\text{Yanai}}(y) \\ 0 \\ \eta_{\text{Yanai}}(y) \\ 0 \\ v_{\text{Yanai}}(y) \\ 0 \end{pmatrix} \propto \begin{pmatrix} \omega E_1(y) \\ 0 \\ k_x E_1(y) \\ 0 \\ (\omega^2 - k_x^2) E_0(y) \\ 0 \end{pmatrix}. \tag{A9}$$

The cross-band coupling of this mixed mode is evident in the frequency-dependent amplitudes, allowing it to interpolate between gravity-like and Rossby-like behavior.

3. **Equatorial Rossby Waves:** These are low-frequency waves that propagate westward and are driven primarily by the spatial variation of the Coriolis parameter β. Governed by higher-order Hermite polynomials $E_n(y)$, with $n \geq 1$, due to the spatial variation of the Coriolis force, the purely westward propagating equatorial Rossby waves are characterized by strong rotational vorticity. The 6d quadrature state for this wave takes the form,

$$\Phi^{(n)}_{\text{Rossby}}(y, k_x) = \begin{pmatrix} u_n(y) \\ 0 \\ \eta_n(y) \\ 0 \\ v_n(y) \\ 0 \end{pmatrix}, \tag{A10}$$

where $v_n(y) \propto E_n(y)$, and the zonal velocity $u_n(y)$ and height anomaly $\eta_n(y)$ are combinations of $E_{n-1}(y)$ and $E_{n+1}(y)$. In this real 6d representation, the topological properties make their spectral flow occupy the negative k_x domain. In other words, the underlying geometry of the rotating planet guarantees that these Rossby waves must exist, and it mathematically forces them to only ever travel westward.

 doi:10.20944/preprints202605.0606.v1

Appendix A.4. Deriving Matsuno's Spatial Envelopes via Real Quadratures

The standard derivation of the equatorial waves relies on substituting a complex wave Ansatz into the shallow water equations. Here we re-derive the spatial envelopes $E_n(y)$ within the real Hilbert space framework.

We begin with the linearized shallow water equations on the equatorial beta-plane, where the Coriolis parameter is expanded as $f = \beta y$,

$$\begin{aligned} \partial_t u - \beta y v + \partial_x \eta &= 0, && \text{(A11)} \\ \partial_t v + \beta y u + \partial_y \eta &= 0, && \text{(A12)} \\ \partial_t \eta + \partial_x u + \partial_y v &= 0. && \text{(A13)} \end{aligned}$$

Instead of a complex phase, we project the physical 3d wave field onto two orthogonal harmonic quadratures. By exploiting the $SO(2)$ Stueckelberg gauge symmetry established in Section 2.3, we lock the zonal velocity and height anomaly into the cosine quadrature, and assign the meridional velocity to the sine quadrature. The real continuous wave field is then defined as

$$\begin{aligned} u(x,y,t) &= U(y)\cos(k_x x - \omega t), && \text{(A14)} \\ v(x,y,t) &= V(y)\sin(k_x x - \omega t), && \text{(A15)} \\ \eta(x,y,t) &= H(y)\cos(k_x x - \omega t). && \text{(A16)} \end{aligned}$$

Here, the spatial profiles $U(y)$, $V(y)$, and $H(y)$ act as the position-dependent amplitude states for our 6d vector $\Phi(y, k_x)$. Substituting this real ansatz into the fluid equations and dividing out the harmonic terms yields a coupled system of purely real ordinary differential equations,

$$\begin{aligned} \omega U - \beta y V - k_x H &= 0, && \text{(A17)} \\ -\omega V + \beta y U + \partial_y H &= 0, && \text{(A18)} \\ \omega H - k_x U + \partial_y V &= 0. && \text{(A19)} \end{aligned}$$

Appendix A.4.1. The Kelvin Wave Envelope

The equatorial Kelvin wave is defined by the absence of North-South flow, setting $V(y) = 0$ everywhere. Substituting this boundary condition into Eq. (A17) and (A19) requires that $\omega U = k_x H$ and $\omega H = k_x U$. This enforces a strictly non-dispersive, eastward-propagating solution where $\omega = k_x$ and $U(y) = H(y)$. Substituting $V = 0$ and $U = H$ into the remaining Eq. (A18) gives,

$$\beta y H + \partial_y H = 0 \implies \frac{\partial H}{\partial y} = -\beta y H. \quad \text{(A20)}$$

Integrating this first-order separable equation generates the fundamental Gaussian decay envelope,

$$H(y) \propto e^{-\frac{\beta y^2}{2}} \equiv E_0(y). \quad \text{(A21)}$$

Appendix A.4.2. The Higher-Order Envelopes and the Harmonic Oscillator

For the Yanai, Poincaré, and Rossby waves, the meridional velocity is non-zero, $V \neq 0$. To find the spatial profiles for these waves, we eliminate $U(y)$ and $H(y)$ to isolate $V(y)$.

Multiplying Eq. (A17) by ω and Eq. (A19) by k_x, then taking their sum, yields an expression for $U(y)$,

$$U(y) = \frac{1}{\omega^2 - k_x^2}(\omega\beta y V - k_x \partial_y V). \quad \text{(A22)}$$

 doi:10.20944/preprints202605.0606.v1

Similarly, multiplying Eq. (A17) by k_x and Eq. (A19) by ω gives $H(y)$,

$$H(y) = \frac{1}{\omega^2 - k_x^2}\left(k_x \beta y V - \omega \partial_y V\right). \tag{A23}$$

We then substitute Eqs. (A22) and (A23) into Eq. (A18),

$$-\omega V + \frac{\beta y}{\omega^2 - k_x^2}\left(\omega \beta y V - k_x \partial_y V\right) + \frac{1}{\omega^2 - k_x^2}\partial_y\left(k_x \beta y V - \omega \partial_y V\right) = 0. \tag{A24}$$

Expanding the derivative in the final term, $\partial_y(k_x \beta y V) = k_x \beta V + k_x \beta y \partial_y V$, cancels the first-order derivatives of V. Multiplying the entire equation by $-(\omega^2 - k_x^2)/\omega$ leaves a single second-order differential equation,

$$\frac{d^2V}{dy^2} + \left[\left(\omega^2 - k_x^2 - \frac{k_x \beta}{\omega}\right) - \beta^2 y^2\right] V = 0. \tag{A25}$$

This is equivalent to the 1d Schrödinger equation for a quantum harmonic oscillator. For the fluid anomalies to remain physically bounded at high latitudes, $y \to \pm\infty$, the constant term inside the brackets must equal an odd integer multiple of β,

$$\omega^2 - k_x^2 - \frac{k_x \beta}{\omega} = \beta(2n + 1), \quad n = 0, 1, 2, \ldots . \tag{A26}$$

This boundary requirement naturally quantizes the dispersion relation for the Yanai ($n = 0$) and Rossby/Poincaré ($n \geq 1$) bands. Because this is the harmonic oscillator equation, its bound eigenstates are the Hermite polynomials $H_n(\sqrt{\beta} y)$ modulated by the ground-state Gaussian. Thus, the 6d quadrature states spontaneously organize into the quantized spatial envelopes,

$$E_n(y) = H_n(\sqrt{\beta} y) e^{-\frac{\beta y^2}{2}}. \tag{A27}$$

Appendix A.5. The Topological Literature

With the basic waves defined, we can trace how physicists have recently connected these classical fluid phenomena to topological quantum mechanics.

1. The topological connection (2017): Delplace, Marston, and Venaille [3] recognized that Matsuno's fluid equations could be mapped onto the Hamiltonian of a topological insulator. They calculated the Chern numbers of the bulk Poincaré bands and applied the bulk-boundary correspondence. This analysis showed that the Kelvin and Yanai waves are not just mathematical solutions, but are topologically guaranteed to exist due to the geometric twisting of the bulk Poincaré waves.

2. The physical questions (2017): In the accompanying perspective, Biello and Dimofte [11] raised two important physical questions about applying quantum topology to classical fluids. First, quantum winding numbers rely on the rotating phase of complex-valued wave functions, but physical fluid waves are inherently real. If we combine complex waves to form real ones, it was unclear why the topological winding numbers would not simply cancel out. Second, quantum electron systems have a Fermi sea (a filled ground state up to a certain energy) that enforces the direction in which edge states must travel. Fluids lack a Fermi sea, leading to the question of what specific mechanism forces the Kelvin wave to travel eastward rather than allowing westward boundary modes.

3. Quantum geometry in fluids (2026): More recently, Ganeshan and Dorsey [10] investigated the detailed quantum geometry of the bulk Poincaré waves, explicitly deriving the complex quantum geometric tensor. Their work clarified the geometric structure of the bulk bands, though it relied on a complex mapping that left the question of real-valued classical waves open.

4. The real and supersymmetric resolution proposal: Finally, this paper addresses the remaining open questions. By reformulating the fluid in a fully real, six-dimensional Stueckelberg parameter space, we find that the Berry curvature is a real symplectic geometric feature, not an artifact of a complex phase. This explains how real classical waves retain their topological winding without

 doi:10.20944/preprints202605.0606.v1

cancellation. Furthermore, by showing that the fluid equations share the mathematical structure of supersymmetric quantum mechanics, we identify the geostrophic zero-modes as an unbroken vacuum state. This vacuum mathematically replaces the quantum Fermi sea, restricting the system's spectral flow and guaranteeing that the boundary modes (Kelvin waves) must travel eastward to bridge the gap between the vacuum and the excited bulk bands.

Appendix B. Proof of Witten's Theorem in the Finite-Dimensional Real Parameter Space

In infinite-dimensional quantum field theories proving the topological invariance of the Witten index can be mathematically delicate due to states escaping to infinity or non-normalizable boundary conditions. However, in our real Stueckelberg formulation of the rotating shallow water model at a fixed wave vector the parameter space is a finite-dimensional real vector space, $\mathbb{R}^6$. In this finite-dimensional regime Witten's theorem becomes a rigorous consequence of the real spectral theorem of linear algebra.

Below we explicitly prove that the Witten index $W = \mathrm{Tr}(\Gamma)$ counts the difference between the number of bosonic and fermionic zero-energy vacuum states in a real Hilbert space, guaranteeing their topological protection.

Definitions

We begin by defining the real, finite-dimensional supersymmetric algebra corresponding to the exact chiral limit of our fluid system (the non-rotating $f = 0$ limit):

1. **The grading operator (Γ):** A real, symmetric involution matrix,

$$\Gamma^{\mathrm{T}} = \Gamma, \quad \Gamma^2 = I_6. \tag{A28}$$

   It partitions the $\mathbb{R}^6$ space into a "bosonic" sector (eigenvalue $+1$) and a "fermionic" sector (eigenvalue -1).
2. **The supercharge ($\mathcal{Q}$):** A real, symmetric matrix,

$$\mathcal{Q}^{\mathrm{T}} = \mathcal{Q}. \tag{A29}$$

3. **Exact chiral symmetry:** In the bare algebra the supercharge anticommutes with the grading operator,

$$\{\Gamma, \mathcal{Q}\} = \Gamma\mathcal{Q} + \mathcal{Q}\Gamma = 0 \implies \Gamma\mathcal{Q} = -\mathcal{Q}\Gamma. \tag{A30}$$

4. **The Hamiltonian ($\mathcal{H}$):** The energy operator is generated directly by the square of the supercharge,

$$\mathcal{H} \equiv \mathcal{Q}^2. \tag{A31}$$

Step 1: Positive semi-definite energy

Let Φ be an arbitrary real state vector in $\mathbb{R}^6$. The expected energy of this state is given by the inner product,

$$E = \Phi^{\mathrm{T}}\mathcal{H}\Phi = \Phi^{\mathrm{T}}\mathcal{Q}^2\Phi. \tag{A32}$$

Because the supercharge is a real symmetric matrix, $\mathcal{Q}^{\mathrm{T}} = \mathcal{Q}$, we may rewrite this as

$$E = \Phi^{\mathrm{T}}\mathcal{Q}^{\mathrm{T}}\mathcal{Q}\Phi = (\mathcal{Q}\Phi)^{\mathrm{T}}(\mathcal{Q}\Phi) = ||\mathcal{Q}\Phi||^2. \tag{A33}$$

Because the dot product of any real vector with itself is non-negative, it follows that $E \geq 0$. In addition, $E = 0$ if and only if $\mathcal{Q}\Phi = 0$, meaning that any zero-energy states are annihilated by the supercharge.

 doi:10.20944/preprints202605.0606.v1

Step 2: Commutation and simultaneous eigenstates

Next, we examine the commutation relation between the grading operator and the energy Hamiltonian,

$$\Gamma\mathcal{H} = \Gamma(\mathcal{Q}\mathcal{Q}) = (\Gamma\mathcal{Q})\mathcal{Q} = (-\mathcal{Q}\Gamma)\mathcal{Q} = -\mathcal{Q}(\Gamma\mathcal{Q}) = -\mathcal{Q}(-\mathcal{Q}\Gamma) = \mathcal{Q}^2\Gamma = \mathcal{H}\Gamma. \tag{A34}$$

Because $\Gamma\mathcal{H} = \mathcal{H}\Gamma$, the operators commute, $[\Gamma, \mathcal{H}] = 0$.

By the real spectral theorem, any set of mutually commuting real symmetric matrices can be simultaneously diagonalized. This guarantees the existence of a complete orthonormal basis of six vectors for $\mathbb{R}^6$, where every basis vector Φ_i is a simultaneous eigenstate of both energy, E_i, and parity, ± 1.

Step 3: Pairing of the strictly positive energy states

Assume there exists a bosonic state Φ_B with strictly positive energy $E > 0$. By definition, $\mathcal{H}\Phi_B = E\Phi_B$ and $\Gamma\Phi_B = (+1)\Phi_B$.

We apply the supercharge to generate a transformed state, $\Psi = \mathcal{Q}\Phi_B$, and test its fundamental properties:

1. **Fermionic parity:** $\Gamma\Psi = \Gamma(\mathcal{Q}\Phi_B) = -\mathcal{Q}(\Gamma\Phi_B) = -\mathcal{Q}(+1\Phi_B) = -\mathcal{Q}\Phi_B = -1\Psi$. The new state is a strict fermion.
2. **Energy preservation:** $\mathcal{H}\Psi = \mathcal{Q}^2(\mathcal{Q}\Phi_B) = \mathcal{Q}(\mathcal{Q}^2\Phi_B) = \mathcal{Q}(E\Phi_B) = E(\mathcal{Q}\Phi_B) = E\Psi$. The new state shares the exact same energy E.
3. **Non-triviality:** $||\Psi||^2 = \Psi^{\mathrm{T}}\Psi = (\mathcal{Q}\Phi_B)^{\mathrm{T}}(\mathcal{Q}\Phi_B) = \Phi_B^{\mathrm{T}}\mathcal{H}\Phi_B = E||\Phi_B||^2$. Because $E > 0$ and Φ_B is not the zero vector, $||\Psi||^2 > 0$, so the state exists.

This establishes a strict bijection. For every single bosonic state with $E > 0$, there exists an exact, linearly independent fermionic state with the identical energy. Therefore, all $E > 0$ states in the finite-dimensional space must exist in degenerate boson-fermion pairs.

Step 4: Topological protection of the Witten index

The Witten index is defined as the trace of the grading matrix,

$$W = \mathrm{Tr}(\Gamma). \tag{A35}$$

Because the trace is invariant under basis transformations, we can evaluate it in our simultaneous eigenbasis. The trace is simply the sum of the Γ eigenvalues for all six basis states,

$$W = \sum_{i=1}^{6} \langle\Phi_i|\Gamma|\Phi_i\rangle. \tag{A36}$$

We partition this sum into states with strictly positive energy and states with zero energy,

$$W = \sum_{E_i>0} \langle\Phi_i|\Gamma|\Phi_i\rangle + \sum_{E_i=0} \langle\Phi_i|\Gamma|\Phi_i\rangle. \tag{A37}$$

Due to the bijection established in Step 3, the states in the first sum occur in pairs of $(+1)$ and (-1). Therefore, the $E > 0$ sector cancels itself out to zero, and we are left with the zero-energy vacuum sector. Defining n_B as the number of zero-energy bosons and n_F as the number of zero-energy fermions, the trace is

$$W = n_B - n_F. \tag{A38}$$

In our specific 6×6 fluid matrix tracing the bare grading operator gives $W = -2$. The proof above guarantees that $n_B - n_F = -2$, guaranteeing the existence of at least two zero-energy vacuum states, $n_F \geq 2$.

 doi:10.20944/preprints202605.0606.v1

When the Coriolis parameter is activated, $f \neq 0$, the matrix elements of $\mathcal{H}$ are deformed, acting as an interaction term that hybridizes the bare bosons and fermions. However, because the dimension of the parameter space remains finite and the trace of a constant grading matrix is impervious to continuous deformations of the Hamiltonian, the exact cancellation holds. The topological index locks the zero-energy states in place, forbidding the steady geostrophic modes from acquiring non-zero frequencies.

Appendix C. Supersymmetry in Standard Complex-Valued Formulation of the Rotating Shallow Water Model

In the main text, we constructed a six-dimensional real Stueckelberg parameter space to identify the topological zero-modes of the rotating shallow water equations via the Witten index. It is highly instructive to demonstrate how this supersymmetric algebra manifests in the standard three-dimensional complex formulation of the fluid, which serves as the foundation for the quantum geometric tensor derivations by Ganeshan and Dorsey [10] and the topological band theory analysis by Delplace *et al.* [3].

In the standard complex formulation, the physical wave anomalies are represented by a three-component complex vector, $\Psi_C = (u, v, \eta)^{\mathrm{T}}$. The linearized equations of motion are cast as a local eigenvalue problem in momentum space, $\omega\Psi_C = \mathcal{H}_C\Psi_C$, where the 3×3 complex, self-adjoint Hamiltonian is given by

$$\mathcal{H}_C = \begin{pmatrix} 0 & -if & k_x \\ if & 0 & k_y \\ k_x & k_y & 0 \end{pmatrix}. \tag{A39}$$

Because this operator is self-adjoint,

$$\mathcal{H}_C^\dagger = \mathcal{H}_C, \tag{A40}$$

it fulfills the role of the fundamental supercharge in a supersymmetric algebra. We therefore identify the complex supercharge as

$$\mathcal{Q}_C \equiv \mathcal{H}_C. \tag{A41}$$

In standard supersymmetric quantum mechanics the energy must be non-negative, so we generate the positive semi-definite SUSY Hamiltonian by squaring this supercharge,

$$\mathcal{H}_{\mathrm{SUSY}}^{(C)} = \mathcal{Q}_C^2 = \begin{pmatrix} k_x^2 + f^2 & k_x k_y & -ifk_y \\ k_x k_y & k_y^2 + f^2 & ifk_x \\ ifk_y & -ifk_x & k^2 \end{pmatrix}. \tag{A42}$$

The eigenvalue spectrum of this operator is

$$E = \omega^2 \in \{0, k^2 + f^2, k^2 + f^2\}, \tag{A43}$$

which matches the unbroken supersymmetric requirement of having a zero-energy vacuum state below a set of doubly-degenerate excited supermultiplets (the high-frequency Poincaré gravity waves).

In order to classify the spectrum topologically we introduce the chiral grading operator, Γ_C. Following the physical correspondence established in our real formulation, we assign the scalar height field η to the bosonic sector $(+1)$ and the vector velocity components u and v to the fermionic sector (-1),

$$\Gamma_C = \begin{pmatrix} -1 & 0 & 0 \\ 0 & -1 & 0 \\ 0 & 0 & 1 \end{pmatrix}. \tag{A44}$$

When the planet is non-rotating, $f = 0$, the pure fluid gradient terms anticommute with the grading operator,

$$\{\Gamma_C, \mathcal{Q}_C\}_{f=0} = 0, \tag{A45}$$

 doi:10.20944/preprints202605.0606.v1

representing an exact chiral symmetry. When planetary rotation is introduced, $f \neq 0$, the Coriolis parameter couples the orthogonal fermions, u and v, acting as a chiral-symmetry-breaking mass term,

$$\{\Gamma_C, \mathcal{Q}_C\} = \begin{pmatrix} 0 & -2if & 0 \\ 2if & 0 & 0 \\ 0 & 0 & 0 \end{pmatrix} \neq 0. \tag{A46}$$

However, as required by the topological invariance of the Witten index, the continuous deformation of the Hamiltonian by the Coriolis mass term cannot alter the number of zero-energy ground states. We may therefore evaluate the Witten index using the bare grading operator,

$$W_C = \mathrm{Tr}(\Gamma_C) = -1. \tag{A47}$$

The index $W_C = -1$ guarantees the existence of $|W_C| = 1$ unbroken zero-energy mode, which corresponds to the single complex geostrophic mode with $\omega = 0$ characteristic of the 3×3 system.

This result emphasizes a nice mathematical correspondence between the standard complex geometry and our real geometry. In the standard 3D complex formulation, the system is described by one complex zero-mode, $W_C = -1$, and one complex pair of excited bulk modes. By unpacking the complex phase into orthogonal $SO(2)$ quadratures the 6D real Stueckelberg formulation doubles the number of degrees of freedom, and the Witten index simply doubles to $W = -2$, predicting the independent real sine and cosine quadratures of the geostrophic balance. Whether analyzed via the 3D complex formulation [10] or via our 6D real formulation, the permanent existence of the planetary zero-frequency geostrophic modes is shown to be a definitive topologically protected feature of the fluid's kinematics.

References

1. B. A. Bernevig and T. L. Hughes, *Topological Insulators and Topological Superconductors* (Princeton University Press, 2013).
2. D. Vanderbilt, *Berry Phases in Electronic Structure Theory: Electric Polarization, Orbital Magnetization and Topological Insulators* (Cambridge University Press, 2018).
3. P. Delplace, J. B. Marston, and A. Venaille, Topological origin of equatorial waves, Science **358**, 1075–1077 (2017).
4. C. Tauber, P. Delplace, and A. Venaille, A bulk-interface correspondence for equatorial waves, J. Fluid Mech. **868**, R2 (2019).
5. N. Perez, A. Leclerc, G. Laibe, and P. Delplace, Topology of shallow-water waves on a rotating sphere, J. Fluid Mech. **1003**, A35 (2025).
6. T. Matsuno, Quasi-geostrophic motions in the equatorial area, J. Meteorol. Soc. Jpn. **44**, 25 (1966).
7. W. Thomson, On gravitational oscillations of rotating water, Proc. Royal Soc. Edinburgh **10**, 92–100 (1880).
8. R. Süsstrunk and S. D. Huber, Observation of phononic helical edge states in a mechanical topological insulator, Science **349**, 47 (2015).
9. L. M. Nash, D. Kleckner, A. Read, V. Vitelli, A. M. Turner, and W. T. M. Irvine, Topological mechanics of gyroscopic metamaterials, Proc. Natl. Acad. Sci. U.S.A. **112**, 14495 (2015).
10. S. Ganeshan and A. T. Dorsey, Quantum geometry of the rotating shallow water model, arXiv:2601.10695 [physics.flu-dyn].
11. J. A. Biello and T. Dimofte, Why do Earth's equatorial waves head east? Science **358**, 990–991 (2017).
12. E. C. G. Stueckelberg, Quantum Theory in Real Hilbert Space, Helv. Phys. Acta **33**, 727 (1960).
13. J. P. Provost and G. Vallee, Riemannian structure on manifolds of quantum states, Commun. Math. Phys. **76**, 289 (1980).
14. R. Cheng, Quantum Geometric Tensor (Fubini-Study Metric) in Simple Quantum System: A pedagogical Introduction, arXiv:1012.1337 [quant-ph].
15. N. Verma, P. J. W. Moll, T. Holder, and R. Queiroz, Quantum geometry and the hidden scales in materials, Nature Reviews Physics **8**, 226–239 (2026).
16. A. Gao, N. Nagaosa, N. Ni, and S.-Y. Xu, Quantum Geometry Phenomena in Condensed Matter Systems, arXiv:2508.00469 [cond-mat.str-el] (2025).

 doi:10.20944/preprints202605.0606.v1

17. J. Yu, B. A. Bernevig, R. Queiroz, E. Rossi, P. Törmä, and B.-J. Yang, Quantum Geometry in Quantum Materials, arXiv:2501.00098 [cond-mat.mes-hall] (2025).
18. G. Fubini, Sulle metriche definite da una forma hermitiana, Atti del Reale Istituto Veneto di Scienze, Lettere ed Arti 63, 501 (1904).
19. E. Study, Kürzeste wege im komplexen gebiet, Math. Ann. 60, 321 (1905).
20. M. V. Berry, Quantal phase factors accompanying adiabatic changes, Proc. R. Soc. Lond. A **392**, 45 (1984).
21. E. Witten, Dynamical breaking of supersymmetry, Nucl. Phys. B **188**, 513 (1981).
22. E. Witten, Constraints on Supersymmetry Breaking, Nucl. Phys. B **202**, 253 (1982).
23. F. Cooper, A. Khare, and U. Sukhatme, Supersymmetry and quantum mechanics, Phys. Rep. **251**, 267 (1995).
24. E. Gozzi, M. Reuter, and W. D. Thacker, Hidden BRS invariance in classical mechanics. II. Phys. Rev. D, **40**, 3363 (1989).
25. D. Tong, A Gauge Theory for Shallow Water, SciPost Phys. **14**, 102 (2023); arXiv:2209.10574 [hep-th]
26. G. K. Vallis, Atmospheric and Oceanic Fluid Dynamics: Fundamentals and Large Scale Applications (2nd ed.) (Cambridge University Press, 2017).
27. V. Zeitlin, Geophysical fluid dynamics: understanding (almost) everything with rotating shallow water models (Oxford University Press, 2018).